

NASA TR R-152

**NATIONAL AERONAUTICS AND  
SPACE ADMINISTRATION**

LOAN COPY  
AFW.  
KIRTLAND  
TECH LIBRARY KAFB, NM  
RN TO  
MEX



**TECHNICAL REPORT  
R-152**

**THE AERODYNAMIC DESIGN OF WINGS WITH CAMBERED  
SPAN HAVING MINIMUM INDUCED DRAG**

By CLARENCE D. CONE, JR.

1963



---

# **TECHNICAL REPORT R-152**

---

## **THE AERODYNAMIC DESIGN OF WINGS WITH CAMBERED SPAN HAVING MINIMUM INDUCED DRAG**

**By CLARENCE D. CONE, JR.**

**Langley Research Center  
Langley Station, Hampton, Va.**



## CONTENTS

	Page
SUMMARY .....	1
INTRODUCTION .....	1
SYMBOLS .....	2
THE DRAG POLAR OF CAMBERED-SPAN WINGS .....	3
PROPERTIES OF CAMBERED WINGS HAVING MINIMUM INDUCED DRAG .....	4
The Optimum Circulation Distribution .....	4
The Effective Aspect Ratio .....	5
THE DESIGN OF CAMBERED WINGS .....	6
Determination of the Wing Shape for Maximum $L/D$ .....	7
Specification of design requirements .....	8
Determination of minimum value of chord function .....	8
Determination of wing profile-drag coefficient and optimum chord function .....	9
The optimum cruise altitude .....	11
The effective downwash distribution at cruise .....	11
Wing twist function for minimum induced drag .....	12
Final wing form .....	12
Additional Design Considerations .....	12
Section profile selection .....	12
Angle-of-attack variations .....	13
Take-off and landing requirements .....	13
Structural considerations .....	14
Special missions .....	14
ILLUSTRATIVE DESIGN OF A CAMBERED-SPAN WING .....	14
Basic Design Conditions .....	15
The Spanwise Camber-Line Geometry .....	15
The Chord Function $c(s)$ .....	17
The Wing Drag Polar for Minimum Induced Drag .....	17
The Optimum Cruise Altitude .....	18
The Effective Downwash at Cruise .....	18
The Twist Function $\theta(s)$ .....	18
The Final Wing Form .....	19
DETERMINATION OF THE WING PITCHING MOMENT .....	21
Pitching Moment of the Most General Wing Form .....	22
The section pitching-moment contribution .....	22
Wing pitching moment about $Y$ -axis .....	23
Wing moment about arbitrary axis .....	23
Pitching Moment of a Wing Constructed of Similar Profiles .....	23
Wing pitching moment about $Y$ -axis .....	23
Pitching moment about an arbitrary axis .....	24
Variation of $C_{m,P}$ With $C_L$ for General Wing Form .....	24
Variation of $C_m$ With $C_L$ for Similar-Profile Wing .....	24
Locus of Trim Axis .....	24
CONCLUDING REMARKS .....	25
APPENDIX A—THE RELATIONSHIP OF LIFT TO INDUCED DRAG FOR OPTIMALLY LOADED AIRFOILS .....	26
REFERENCES .....	26

## TECHNICAL REPORT R-152

# THE AERODYNAMIC DESIGN OF WINGS WITH CAMBERED SPAN HAVING MINIMUM INDUCED DRAG

By CLARENCE D. CONE, JR.

### SUMMARY

*The basic aerodynamic relations needed for the design of wings with cambered span having a minimum induced drag at specified flight conditions are developed for wings of arbitrary spanwise camber. Procedures are also developed for determining the physical wing form required to obtain the maximum value of lift-drag ratio at cruise, when the wing spanwise camber-line and section profiles are specified, by optimizing the wing chord and twist distributions with respect to both profile and induced drags.*

*The application of the design procedure is illustrated by determining the physical wing form for a circular-arc spanwise camber line. The efficiency of this cambered wing is compared with that of an equal-span, flat wing of elliptical planform which satisfies the same set of flight operating conditions as does the cambered wing.*

*The wing pitching-moment equations for optimally loaded cambered-span wings at design flight conditions are also developed for use in trim analyses on complete aircraft designs.*

### INTRODUCTION

The theoretical considerations of reference 1 indicated that the reduction in induced drag attainable with optimally loaded, nonplanar lifting systems might allow some gain in wing aerodynamic efficiency (lift-drag ratio) over that of flat wings when the lateral span of the wing system is limited by operational requirements. In particular, it was shown that substantial increases in effective aspect ratio (as compared with that of flat wings of equal projected span) could be obtained with relatively simple wing forms having cambered spans, that is, wings in which the span

has curvature in a plane perpendicular to the direction of flight. Reference 1 pointed out, however, that the practical realization of a net efficiency increase would depend in considerable measure upon the ability to construct cambered wings with profile-drag coefficients and structural weights which would not greatly exceed those of the equivalent flat-span wing producing the same lift. Otherwise, the benefits of the increased effective aspect ratio attainable with camber might be cancelled by increased profile drag, and an increased operational lift force.

The aforementioned effective-aspect-ratio properties of cambered-span airfoils were derived by a theoretical treatment of the ideal vortex systems necessary for minimum induced drag, without consideration of the physical wing forms needed to obtain the optimum distributions of vorticity. In order to investigate the overall performance gains obtainable with such airfoils, the details of the physical wing design must be considered. These details include not only aerodynamic factors but also the effects of the wing structural weight on the operational efficiency (ref. 1). In general, however, structural weight effects can be taken into account after the aerodynamic design of the wing is specified. The purpose of this analysis, consequently, is to develop the general relations needed for the aerodynamic design and efficiency evaluation of airfoils which have arbitrarily specified camber forms (such as circular-arc spanwise segments and semiellipse curves) and which possess minimum induced drag at specified flight conditions, without regard to structural weight effects. The methods by which the optimum lift loading, corresponding to the minimum induced drag of a given spanwise camber line, can be determined

are presented in reference 1. The relations are developed in a form which permits a direct efficiency comparison to be made between an elliptically loaded flat span wing and an optimally loaded (minimum induced drag) wing of arbitrary camber having an equal projected span and producing the same lift force. Thus, in addition to prescribing the wing shape necessary for minimum induced drag with a given camber form under specified flight conditions, the results also show the relative efficiency of the complete cambered wing. The results may be used to investigate the maximum values of lift-drag ratio attainable with any given camber form for any prescribed set of flight operating conditions.

Although the intention of this paper is to discuss only the general design procedure for wings with arbitrary camber, without consideration of the comparative efficiencies of any specific camber shapes, actual calculations are presented for a wing having a circular-arc camber line, in order to illustrate the design procedures and to indicate the order of magnitude of the lift-drag ratio attainable for a particular set of operating conditions.

Consideration is given herein only to the design of the basic cambered wing. In the design of a complete aircraft, the entire vehicle configuration must of course be considered and the parasite drag of the fuselage and other components introduced into the design calculations. However, the procedures outlined herein specifically for wing design are easily adapted to a complete aircraft design by proper inclusion of all the component drag coefficients. In addition, the relations discussed apply equally well in principle to the design of more complex wing forms such as those having compound camber, or branched tips (ref. 1), as well as to the design of low-drag hydrofoils. Because of the restricted allowable span length of most hydrofoil systems, the use of cambered-span hydrofoils appears advantageous as a means for reducing both the induced drag and support-strut drag of conventional systems. The curvature of such hydrofoils might also allow some reduction in free-surface effects. The theoretical basis and practical application aspects of cambered-span wings are discussed in reference 1.

When the use of cambered-span wings is considered for specific aircraft designs, a knowledge

of the pitching-moment characteristics of such wings is of considerable importance. The curvature of the span results in a vertical distribution of the drag forces and this distribution in turn affects the wing pitching moment. A quantitative knowledge of this effect is necessary if the aircraft is to be designed to possess desirable longitudinal trim characteristics. Consequently, the subsequent section "Determination of the Wing Pitching Moment" presents the development of the various aerodynamic relations needed for determining the pitching moment of optimally loaded cambered-span wings for any arbitrary pitch-axis location. These relations are essentially confined to the calculation of the pitching moment of the optimum wing form at specified cruise conditions.

### SYMBOLS

$A$	aspect ratio
$B$	constant, $\int_{-1}^1 \frac{\Gamma}{\Gamma_0} d\gamma$
$b$	wing span of flat reference wing
$b'$	projected wing span of cambered-span wing
$C_D$	wing total-drag coefficient
$C_{D,i}$	wing induced-drag coefficient
$C_{D,o}$	wing profile-drag coefficient
$c_d$	section drag coefficient
$C_L$	wing lift coefficient
$C_{L}^*$	wing lift coefficient for $(L/D)_{max}$
$c_l$	section aerodynamic-force (lift) coefficient
$c_l^*$	section aerodynamic-force coefficient for wing $(L/D)_{max}$
$c_{m,P}$	wing pitching-moment coefficient about arbitrary axis through point $P$
$c$	wing chord
$\bar{c}$	mean aerodynamic chord of flat wing
$c_o$	wing root chord
$D$	wing total drag force
$D'$	wing total drag force intensity (force per unit length)
$D_i'$	wing induced drag force intensity, $\rho w \Gamma$
$d$	spanwise-camber depth (fig. 3)
$F'$	aerodynamic-force loading intensity (fig. 7)

$$f = qD_i \left(\frac{b'}{L}\right)^2$$

$G$	constant, $\int_{-1}^1 \frac{\Gamma}{\Gamma_o} \sec \tau d\gamma$
$h$	flight altitude
$k$	induced drag efficiency factor
$L$	wing lift force
$L'$	lift-force intensity (force per unit length)
$M$	wing pitching moment
$M'$	section pitching moment
$m$	constant, $\frac{S}{c_o B \frac{b}{2}}$
$N_A$	constant, $\frac{\Gamma_o/w_o}{b'/2}$
$q$	dynamic pressure
$r$	radius of curvature of circular arc
$S$	wing area of flat reference wing
$S'$	wing area of cambered-span wing, $\int_{-s_t}^{s_t} c(s) ds$
$s$	arc-span coordinate (fig. 2)
$s_t$	arc-tip coordinate
$V$	flight velocity
$W$	weight force
$w$	effective downwash velocity
$w_o$	downwash velocity at center of span
$x$	Cartesian coordinate in free-stream direction
$x_P$	longitudinal coordinate of arbitrary axis
$y, z$	Cartesian coordinates of spanwise camber line $z(y)$
$y'$	dummy variable of integration
$z'$	distance of line-of-action of $D_o'$ above $Y$ -axis
$z_P$	$z$ -coordinate of arbitrary axis
$z_T$	coordinate of trim axis
$\alpha$	geometrical angle-of-attack function
$\alpha'$	effective angle of attack
$\alpha'^*$	effective angle of attack for $(L/D)_{max}$
$\alpha_i$	induced angle-of-attack function
$\alpha_o$	geometrical angle of attack of wing root section
$\beta$	camber factor, $\frac{d}{b'/2}$

$\Gamma$	wing circulation distribution
$\Gamma_o$	circulation of wing root section
$\gamma$	nondimensional coordinate, $\frac{y}{b'/2}$
$\delta$	nondimensional coordinate, $\frac{z}{b'/2}$
$\theta$	wing twist function
$\rho$	atmospheric density
$\rho_{s_i}$	atmospheric density at sea level
$\sigma$	atmospheric density ratio, $\rho/\rho_{s_i}$
$\tau$	slope of camber-line tangent, $\tan^{-1} \frac{dz}{dy}$
$\psi$	span ratio, $b/b'$

Subscripts:

$C$	condition at cruise
$c/4$	about quarter-chord point of section
$f$	flat-span wing
$L$	condition at landing
$max$	maximum
$o$	in plane of symmetry
$P$	arbitrary axis location
$T$	trim-axis location
$Y$	moment about $Y$ -axis

Parentheses ( ) are used throughout to denote the independent variable of the function preceding the parentheses and should not be interpreted to mean multiplication. Example:  $\frac{\Gamma}{\Gamma_o}(s)$  denotes

that  $\frac{\Gamma}{\Gamma_o}$  is a function of  $s$ .

**THE DRAG POLAR OF CAMBERED-SPAN WINGS**

In reference 1 the relation between the lift coefficient and the induced drag coefficient for any cambered-span wing is expressed as

$$C_{D,i} = \frac{C_L^2}{\pi k A} \quad (1)$$

where the lift coefficient  $C_L$  and aspect ratio  $A$  are based on the span length and wing area of a flat, elliptical-planform wing arbitrarily chosen as a basis for determining the induced drag of the cambered wing. The factor  $k$  is an efficiency factor which determines the maximum effective aspect ratio  $kA$  of the curved wing and is shown to depend only upon the geometrical form and

length of the camber line when the wing possesses the optimum spanwise distribution of circulation  $\frac{\Gamma}{\Gamma_o}(s)$  corresponding to minimum induced drag. The value of  $k$  is given by

$$k = \frac{1}{\pi\psi^2} \frac{\Gamma_o/w_o}{b'/2} \int_{-1}^1 \frac{\Gamma}{\Gamma_o} d\gamma \quad (2)$$

In this equation  $\psi$  is the ratio of the span  $b$  of the reference flat wing to the projected span  $b'$  of the curved wing, and  $\gamma = \frac{y}{b'/2}$  is the nondimensional abscissa coordinate of the camber line (fig. 1).

Thus, if a flat-span, elliptical-planform wing of span  $b$  and area  $S$  is arbitrarily specified, the corresponding lift and drag coefficients of any cambered-span wing can be determined and the total drag polar of the curved wing can be expressed as

$$C_D = C_{D_o} + \frac{C_L^2}{\pi k A} \quad (3)$$

where  $C_{D_o}$  is also based upon the wing area  $S$ . In effect, then, the cambered wing is aerodynamically equivalent to a flat wing of area  $S$ , aspect ratio  $kA$ , and profile-drag coefficient  $C_{D_o}$ . The value of the profile drag coefficient  $C_{D_o}$  of course depends upon the physical surface area and form of the cambered wing at the corresponding lift condition. In the following considerations, the factor  $\psi$  is assigned the constant value 1.0, which means that the coefficients of the cambered wings are being based on a flat wing of equal span,  $b=b'$ . The significance of the factor  $\psi$  is fully discussed in reference 1.

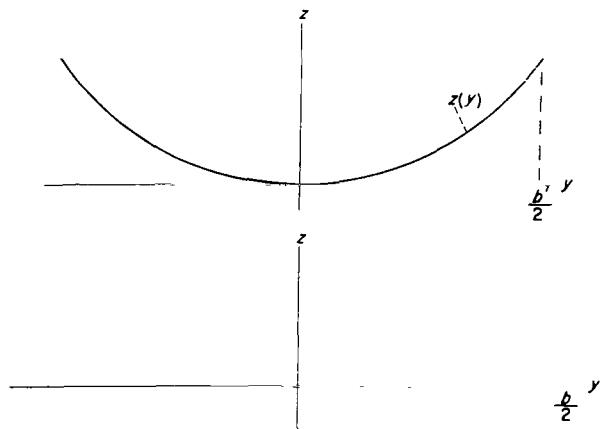


FIGURE 1.—Geometry definitions of flat and cambered-span lifting lines.

In equation (2),  $k$  is a dimensionless constant for the optimum lift distribution and each of its three main factors is also dimensionless, so that the expression for  $k$  may be simplified to the form

$$k = \frac{N_A B}{\pi} \quad (\psi=1.0) \quad (4)$$

where

$$N_A = \frac{\Gamma_o/w_o}{b'/2} \quad (5)$$

$$B = \int_{-1}^1 \frac{\Gamma}{\Gamma_o} d\gamma \quad (6)$$

The factors  $N_A$  and  $B$  are constants for any particular camber-line shape and apply only to the condition of optimum circulation loading for minimum induced drag. The factor  $B$  depends upon the form of the optimum circulation distribution, and  $N_A$  depends upon the circulation-downwash ratio, which is also purely a function of the arc curvature.

By use of equation (3), the aerodynamic efficiency parameter  $L/D$  (and  $\frac{L^{3/2}}{D}$ ) can be established, within the limitations of linear airfoil theory, for any cambered-span wing. This efficiency index can then be directly compared with that obtainable with optimally loaded flat-span wings.

### PROPERTIES OF CAMBERED WINGS HAVING MINIMUM INDUCED DRAG

#### THE OPTIMUM CIRCULATION DISTRIBUTION

For any curved wing form having a spanwise camber line specified by the symmetrical, dimensional function  $z(y)$  (fig. 2), the span must possess a specific circulation distribution  $\frac{\Gamma}{\Gamma_o}(s)$  if the induced drag is to be a minimum at a given lift. This optimum circulation distribution can be

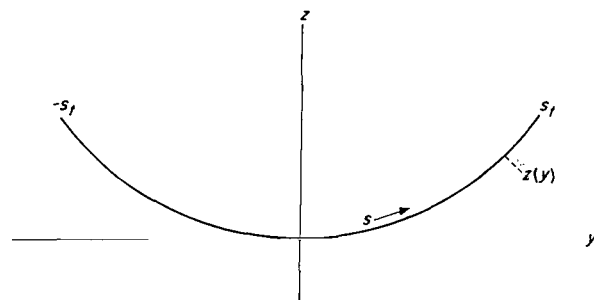


FIGURE 2.—Cambered-span lifting line.

determined by either the conformal-transformation or the electrical-analog technique discussed in reference 1. These methods can also be used to determine the value of  $N_A$  (eq. (5)), and integration of the nondimensional circulation loading  $\Gamma/\Gamma_0$ , determines the value of  $B$  (eq. (6)). For families of camber lines such as circular-arc segments or semiellipses, the optimum distribution  $\Gamma/\Gamma_0$ , and the constants  $N_A$  and  $B$  can be expressed as functions of the camber factor  $\beta$  which describes the particular arc members. (See fig. 3.) The

optimum nondimensional circulation loadings and corresponding values of  $N_A$  and  $B$  are presented in figures 4 and 5 as functions of  $\beta$  for circular and semielliptic arcs, respectively, in order to illustrate the loading variation with camber for simple arc forms. The distribution  $\Gamma/\Gamma_0$  for the case  $\beta=0$  in each figure corresponds to the loading for a flat wing, and it is evident that the effect of camber is to increase the relative loading of the outer portion of the projected span.

**THE EFFECTIVE ASPECT RATIO**

When the values of  $N_A$  and  $B$  have been determined for a given camber line  $z(y)$ , the value of the efficiency factor  $k$  can be calculated by equation (2), for  $\psi=1.0$ . Since the effective aspect ratio of a cambered-span wing is then equal to  $kA$ , where  $A$  is the aspect ratio of the reference elliptical wing of equal span, the induced drag of the curved wing will be less than that of the flat wing for equal lifts when  $k>1$ . This result, of course, is dependent on the assumption that the curved span is optimally loaded at all values of the lift coefficient. The variation of the span efficiency factor  $k$  with degree of camber  $\beta$  is

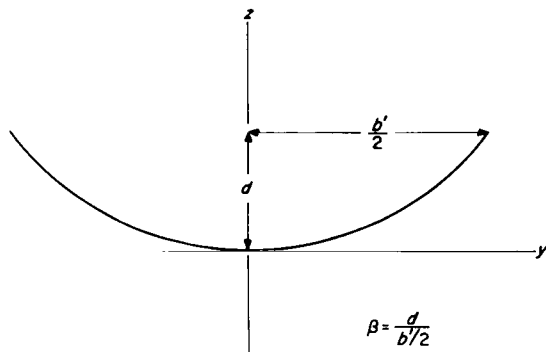


FIGURE 3.—Definition of camber factor  $\beta$ .

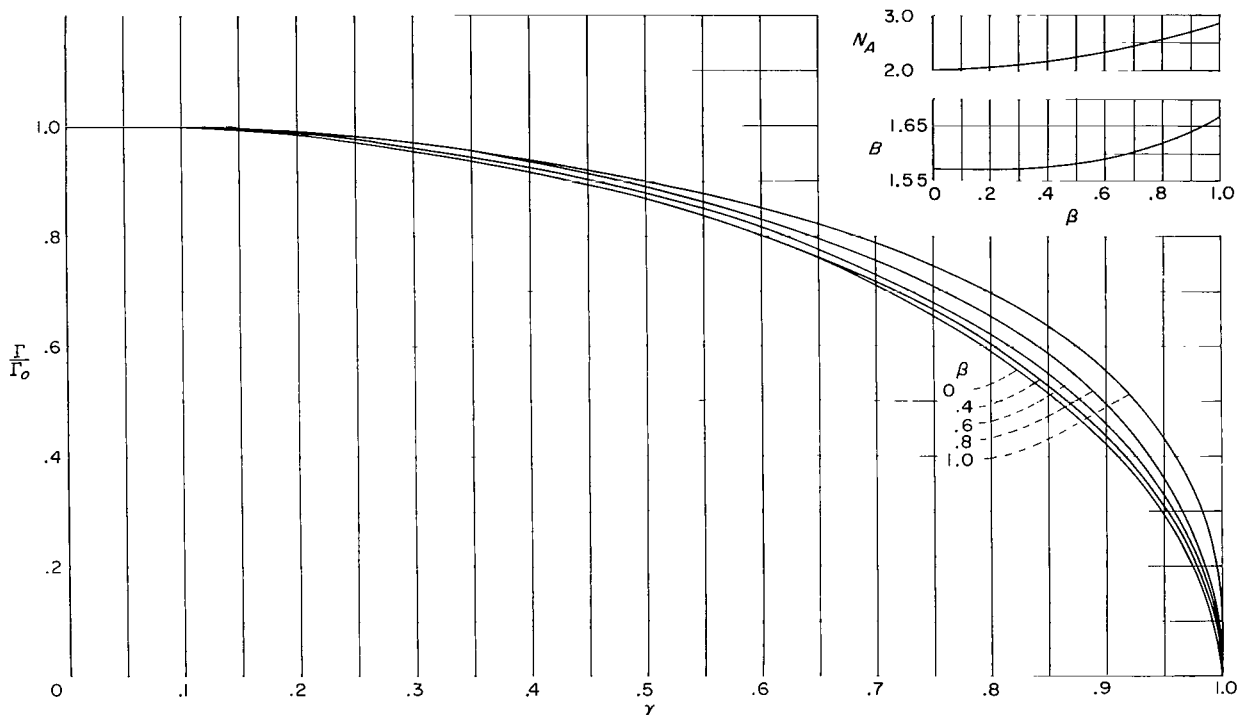


FIGURE 4.—Variation of the optimum nondimensional circulation distribution and efficiency constants of circular-arc camber lines with degree of camber.

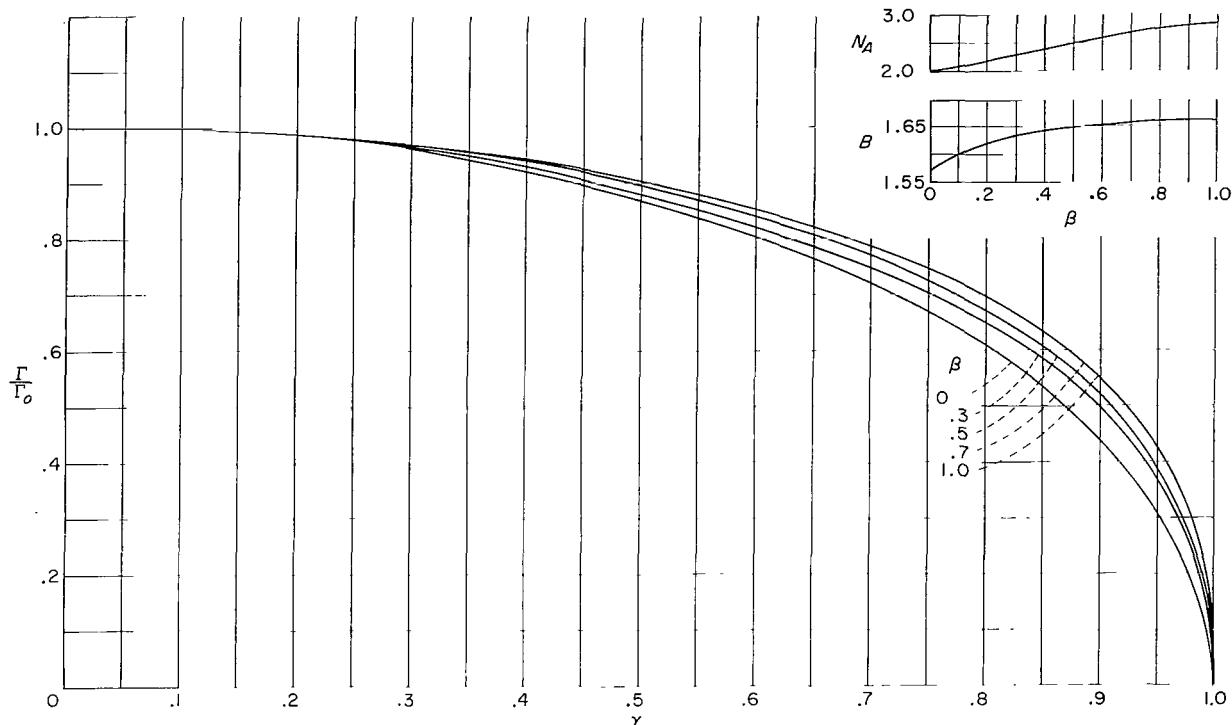


FIGURE 5.—Variation of the optimum nondimensional circulation distribution and efficiency constants of semiellipse camber lines with camber factor  $\beta$ .

presented in figure 6 for the complete families ( $0 \leq \beta \leq 1$ ) of circular-arc segments and semiellipses for the condition  $\psi = 1.0$ .

The following considerations of cambered-span wings are divided into three parts. The first part presents a development of the relations necessary for designing wings which will possess a maximum value of  $L/D$  (for the imposed structural restraints) for specified flight conditions. The second part presents actual calculations for a wing with circular-arc camber as an illustration of the design procedure, and as an indication of the magnitude of the efficiency obtainable with cambered wings. The third part presents relations for determining the wing pitching moments at design flight conditions.

#### THE DESIGN OF CAMBERED WINGS

Consider first a flat reference wing of elliptical planform which is specified by stating its span  $b$ , wing area  $S$ , and constituent section profiles. The aspect ratio is then also determined,  $A = b^2/S$ . The force coefficients are given by

$$C_L = \frac{L}{\frac{1}{2} \rho V^2 S} \quad (7)$$

$$C_{D,f} = C_{D,o,f} + \frac{C_L^2}{\pi A} \quad (8)$$

These equations in turn can be used to determine the wing efficiency parameter  $L/D$  as a function of  $C_L$ .

Consider now an optimally loaded, cambered-span wing of projected span length  $b'$  equal to that of the flat wing and producing an equal lift at the same dynamic pressure  $\frac{1}{2} \rho V^2$ . This cambered wing can have any desired combination of wing twist, chord distribution, and section profile variation, subject only to the requirement that at the prescribed flight conditions under consideration the wing possesses the optimum circulation loading  $\Gamma(s)$  for which the maximum efficiency factor  $k$  applies. If the wing area  $S$  of the reference flat wing is used as the basis for determining the force coefficients of this cambered-span wing, there results

$$C_L = \frac{L}{\frac{1}{2} \rho V^2 S} \quad (9)$$

$$C_D = C_{D_o} + \frac{C_L^2}{\pi k A} \quad (10)$$

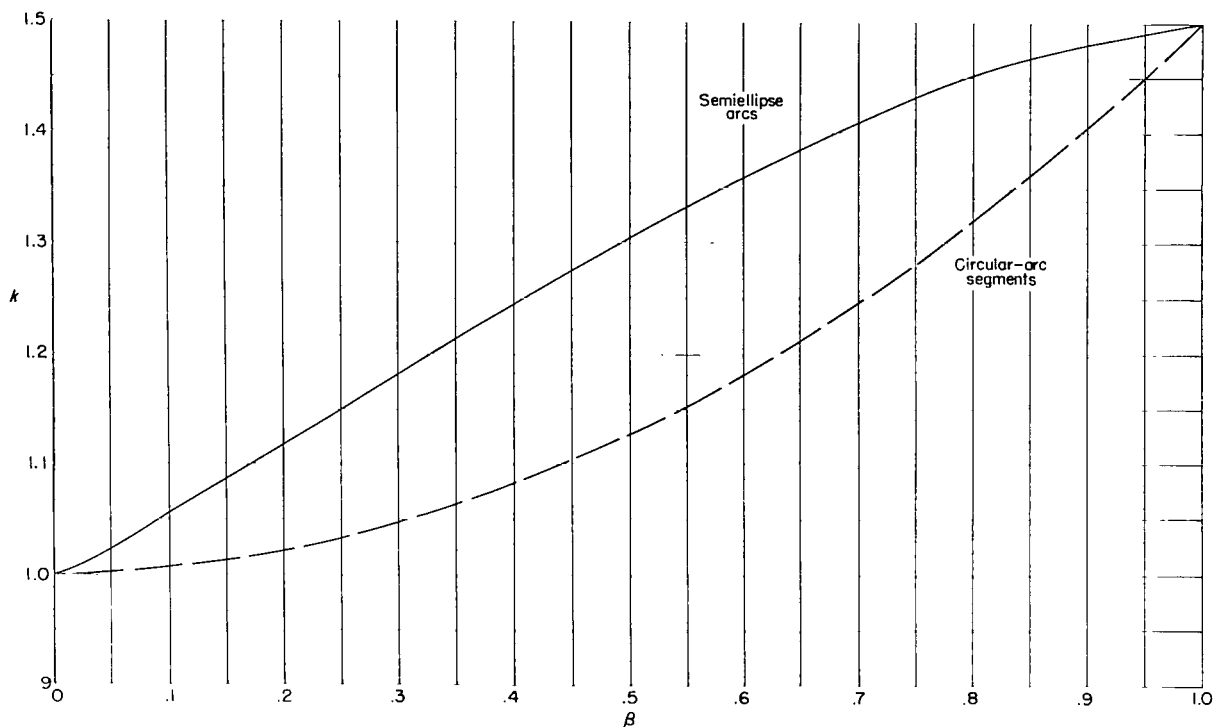


FIGURE 6.—Variation of the efficiency factor  $k$  of circular and semiellipse arcs with the camber factor  $\beta$ .

These coefficients now determine the lift-drag ratio  $L/D$  for the cambered wing.

A comparison of equations (8) and (10) indicates that the cambered-span wing can attain a higher total aerodynamic efficiency than the flat wing at equal lift values if  $k > 1.0$ , provided of course that  $C_{D_o}$  is not proportionately larger than  $C_{D_o,f}$ . Because  $C_{D_o}$  depends critically upon the wing section profiles and physical wing surface area, the ability to realize the full induced-drag efficiency gains offered by spanwise camber obviously rests upon the possibility of constructing curved wings with relatively small surface areas or low drag profiles or both. As is discussed subsequently, a considerable latitude exists for designing wings that possess low values of  $C_{D_o}$  at specified flight conditions, since the value of  $k$  depends only upon the attainment of the optimum circulation loading  $\Gamma(s)$  and is independent of the physical means for obtaining this distribution.

It should be noted that the use in this analysis of a given flat wing as the basis for determining the coefficients of the cambered wing is purely arbitrary and is valuable primarily for efficiency comparison purposes. In reality, any area  $S$  could be used to define the force coefficients of the

cambered wing. The induced drag of a flat, elliptically loaded wing is of course independent of the physical wing area and hence of the physical aspect ratio for a given span and lift, as can be seen from the fundamental relation

$$D_i = \frac{L^2}{\pi q b^2} \quad (11)$$

This fact is discussed in some detail in reference 2, pages 32 and 33, and in appendix A of this report.

#### DETERMINATION OF THE WING SHAPE FOR MAXIMUM $L/D$

The first step in the design procedure is the specification of the nondimensional camber function  $\delta(\gamma)$  where  $\delta = \frac{z}{b'/2}$  and  $\gamma = \frac{y}{b'/2}$ . This function then becomes the corresponding dimensional camber line  $z(y)$  when the projected span length  $b'$  is given. Obviously, the particular value of  $b'$  to be used for a given design depends entirely upon criteria associated with the requirements of the specific aircraft mission, and hence no general procedure can be stated for determining its selection. Once the camber line  $\delta(\gamma)$  or  $z(y)$  is specified, the values of  $k$ ,  $N_A$ , and  $B$ , and the function  $\frac{\Gamma}{\Gamma_0}(s)$

corresponding to minimum induced drag can be determined.

The next step is the selection of the area  $S$  of the flat reference wing of span  $b$  ( $=b'$ ) to be used as a basis for the coefficients. The choice of equal span lengths as a basis for comparison rests upon the fundamental importance of the span in determining the induced drag. (See eq. (A1) and ref. 1.) While the value of the area  $S$  is purely arbitrary, it is convenient to use the value of  $S$  corresponding to that of the "optimum" flat wing which best satisfies the requirements of the specific mission for which the curved wing is being designed. Then the aerodynamic efficiency of the resulting curved wing can be directly compared with that of the optimum flat wing.

**Specification of design requirements.**—In order to design the wing for practical flight operations, certain basic design requirements must be specified. These requirements will determine, to some extent, the design procedure. For the purposes of this analysis, however, the design requirements are taken as the speed  $V_L$  corresponding to the desired landing speed, the load  $W_L$  corresponding to the total weight supported by the wing at landing, the design cruise speed  $V_C$ , and the initial cruise weight  $W_C$ . These criteria are of course arbitrary but serve as a basis for development of the general design relations. Since the landing speed in general is low compared with the cruise speed (depending upon the particular aircraft mission), the landing speed then determines the minimum physical area of a cambered-span wing. Under certain conditions, take-off speed and weight rather than landing speed and weight may be the governing factors.

**Determination of minimum value of chord function.**—A cambered-span wing is usually designed to possess its maximum value of  $L/D$  at some specific cruise flight condition, and the physical form of the wing is therefore such that the optimum circulation distribution for minimum induced drag is obtained. That is, the wing is designed primarily for optimum efficiency at cruise. It is assumed for this analysis, however, that by a proper use of wing flaps or other variable chordwise camber devices, the optimum nondimensional circulation distribution  $\frac{\Gamma}{\Gamma_o}(s)$  can also be obtained (approximately) at landing conditions. Then the values of  $N_A$  and  $B$  apply to both basic flight con-

ditions. Thus the optimum distribution  $\Gamma/\Gamma_o$  can be used in conjunction with the landing requirements to determine the minimum allowable chord distribution of the wing.

In terms of the nondimensional coordinate  $\gamma=y/(b'/2)$ , the lift force at any flight condition

$$L = \rho V \frac{b'}{2} \int_{-1}^1 \Gamma(\gamma) d\gamma \quad (12)$$

becomes, when equation (6) is used,

$$L = \rho V \Gamma_o \frac{b'}{2} B \quad (13)$$

for the design flight and landing conditions. For landing,  $L=W_L$  and  $V=V_L$ , so that

$$\Gamma_{o,L} = \frac{W_L}{\rho_L V_L \frac{b'}{2} B} \quad (14)$$

Here  $\Gamma_{o,L}$  is the circulation in the plane of symmetry of the wing at landing. Since  $\frac{\Gamma}{\Gamma_o}(s)$  can be established by the methods of reference 1, the dimensional circulation distribution  $\Gamma(s)$  along the arc span can be determined as

$$\Gamma_L = \frac{\Gamma}{\Gamma_o} \Gamma_{o,L} \quad (15)$$

The aerodynamic-force loading intensity  $F'$  along the camber line (fig. 7) is given by

$$F'(s) = \rho V \Gamma(s) \quad (16)$$

The corresponding section "lift" coefficient variation  $c_l$  (actually  $c_l$  determines the aerodynamic-

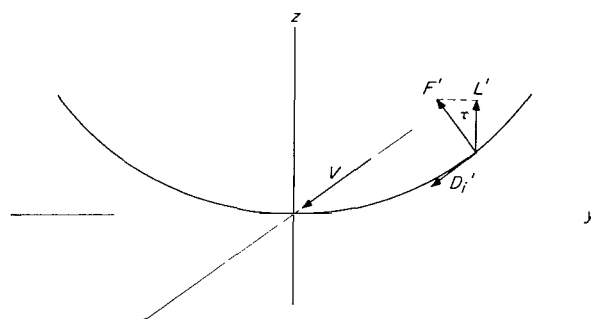


FIGURE 7.—Aerodynamic-force loading intensity and its relation to lift intensity.

force intensity) is given by

$$c_i = \frac{F'(s)}{qc} = \frac{\rho V \Gamma(s)}{\frac{1}{2} \rho V^2 c(s)} \quad (17)$$

and equations (14), (15), and (17) give the chord distribution for the landing condition as

$$c(s) = \frac{W_L}{\frac{1}{2} \rho_L V_L^2 c_{i,L}} \frac{b'}{2} \frac{\Gamma}{\Gamma_0}(s) \quad (18)$$

This equation, upon specification of the function  $c_{i,L}$ , determines the necessary chord distribution and minimum allowable physical surface area of the wing as set by the landing requirements. Obviously, the minimum allowable value of the "effective" wing area  $S'$  is determined by the maximum allowable value of  $c_{i,L}$ , where

$$S' = \int_{-s_t}^{s_t} c(s) ds \quad (19)$$

It also follows from equation (18) that if each section profile is operated at the same value of  $c_{i,L}$ , the chord distribution  $c(s)$  is uniquely determined by the camber-line geometry  $z(y)$  since  $\frac{\Gamma}{\Gamma_0}(s)$  is a function only of the arc shape.

Although equation (18) determines the minimum value of the allowable chord length which still satisfies the landing requirements, this distribution is not necessarily the optimum one corresponding to the maximum value of  $L/D$  for the wing at a given lift coefficient  $C_L$ , since the profile drag is critically dependent upon the actual section chord length. Thus, if the wing is to operate at the maximum possible value of  $L/D$  at a given lift coefficient, the chord distribution must be optimized so as to have minimum profile drag. This optimization procedure is considered next. If the optimum chord distribution is less than that required for landing, the limiting distribution as given by equation (18) must of course be used.

The general form of equation (18) for any flight condition for which the induced drag is to be minimum and in which  $W$ ,  $\rho$ , and  $V$  are specified is

$$c(s) = \frac{W}{\frac{1}{2} \rho V^2} \frac{b'}{2} \frac{\Gamma}{\Gamma_0}(s) \quad (20)$$

**Determination of wing profile-drag coefficient and optimum chord function.**—When a wing section profile is selected, the section drag polar  $c_d(c_i)$  and the section aerodynamic-force curve  $c_i(\alpha')$  are specified. The wing profile-drag coefficient is then given by

$$C_{D_0} = \frac{1}{S} \int_{-s_t}^{s_t} c_d c(s) ds \quad (21)$$

where  $c_d$  is the section drag coefficient corresponding to the operating value of  $c_i$  of the section. The drag coefficient as given by equation (21) does not, of course, include any of the effects such as tip-drag and profile-drag changes which may occur with the curved, three-dimensional wing. If it is anticipated that such effects will be significant, an additive term can be applied in equation (21) to account for them. Assume now that the wing is constructed entirely of similar profiles all of which are operating at the same value of  $c_i$ ; the total wing profile-drag coefficient is then

$$\begin{aligned} C_{D_0} &= \frac{c_d}{S} \int_{-s_t}^{s_t} c(s) ds \\ &= c_d \frac{S'}{S} \end{aligned} \quad (22)$$

The total wing-drag coefficient then becomes

$$C_D = c_d(c_i) \frac{S'}{S} + \frac{C_L^2}{\pi k A} \quad (23)$$

In this equation the profile-drag term appears as a function of  $c_i$ , where  $c_i$  is the section "lift" coefficient corresponding to any given flight condition. Since, however, the wing is being designed for maximum  $L/D$  at cruise,  $c_d$  must now be expressed as a function of  $C_L$  (the total lift coefficient) so that the function  $\frac{L}{D}(C_L)$  can be determined.

The relation between  $c_i$  and  $C_L$  is established by substituting the general weight expression

$$W = C_L \frac{1}{2} \rho V^2 S \quad (24)$$

into equation (20), and after rearrangement the desired relation is obtained as

$$c_i = \left[ \frac{S}{cB} \frac{\Gamma}{\Gamma_0} \right] C_L \quad (25)$$

Since the factor in brackets is a constant, the relation between the section and total wing-lift coefficients can be expressed simply as

$$c_l = m C_L \quad (26)$$

where

$$\begin{aligned} m &= \frac{S}{c_o B} \frac{\Gamma}{b' \Gamma_o} \\ &= \frac{S}{c_o B} \frac{b'}{2} \end{aligned} \quad (27)$$

The individual factors  $\Gamma/\Gamma_o$  and  $c$  are of course functions of the arc-span coordinate  $s$  but their ratio is a constant when each wing section is operated at the same value of  $c_l$ . (See eq. (20).) The total wing-drag coefficient can be expressed as

$$C_D = c_d(m C_L) \frac{S'}{S} + \frac{C_L^2}{\pi k A} \quad (28)$$

In order to determine the chord distribution that will make  $C_D$  a minimum for a given value of  $C_L$ , it is necessary to find the optimum value of the root chord  $c_o$ . The optimum chord-length distribution at that  $C_L$  will then be given by

$$c(s) = c_o \frac{\Gamma}{\Gamma_o}(s) \quad (29)$$

In order to find this optimum value of  $c_o$ , the wing profile-drag coefficient

$$C_{D_o} = c_d(m C_L) \frac{S'}{S} \quad (30)$$

must be expressed as a function of  $c_o$ . From equation (27),

$$m = \frac{S}{c_o B} \frac{b'}{2} \quad (31)$$

and substitution of  $c(s)$  from equation (29) yields

$$\begin{aligned} S' &= \int_{-s_t}^{s_t} c(s) ds \\ &= c_o \int_{-s_t}^{s_t} \frac{\Gamma}{\Gamma_o}(s) ds \end{aligned} \quad (32)$$

Since the second integral is a constant for any particular camber line when it is optimally loaded,

equation (32) can be written as

$$S' = \frac{b'}{2} G c_o \quad (33)$$

where

$$G = \int_{-1}^1 \frac{\Gamma}{\Gamma_o} \sec \tau d\gamma \quad (34)$$

Substituting these values into equation (28) yields as the drag polar

$$C_D = c_d \left( \frac{S}{c_o B} \frac{b'}{2} C_L \right) \frac{G c_o}{S} \frac{b'}{2} + \frac{C_L^2}{\pi k A} \quad (35)$$

where it should be noted that the factor in parentheses is the value of  $c_l$  for which  $c_d$  is to be evaluated; it is a functional relation and not a multiplication factor. The equation for  $L/D$  as a function of  $c_o$ , for a constant value of  $C_L$ , is given by

$$\frac{L}{D} = \frac{C_L}{c_d \left( \frac{S C_L}{c_o B} \frac{b'}{2} \right) \frac{G c_o}{S} \frac{b'}{2} + \frac{C_L^2}{\pi k A}} \quad (36)$$

Now if the section drag polar of the selected profile is used, a plot can be made at constant  $C_L$  of the variation of  $L/D$  with  $c_o$ , and the value of  $c_o$  for which  $L/D$  becomes a maximum determines the optimum chord distribution for that operational value of  $C_L$ . When this procedure is carried out for a range of  $C_L$  values, a plot of  $L/D$  against  $C_L$  will determine the optimum cruise lift coefficient  $C_L^*$  corresponding to the absolute maximum value of wing  $L/D$ , denoted by  $(L/D)_{max}$ , and the corresponding value of  $c_o$ . Then, from equation (30) the profile-drag coefficient at cruise is given by

$$C_{D_o} = c_d(m C_L^*) \frac{S'}{S} \quad (37)$$

where  $S'$  of course depends upon the corresponding optimum value of  $c_o$ .

Since the foregoing procedure determines the optimum chord distribution not only for the optimum cruise condition ( $C_L^*$  and  $(L/D)_{max}$ ) but for the entire lift-coefficient range as well, the wing dimensions for maximum  $L/D$  at any other value of  $C_L$  are also specified.

It should perhaps be emphasized that the relation between  $L/D$  and  $C_L$  as given by equation (36) for the optimum value of  $c_o$  at each  $C_L$  is not the variation of a particular wing  $L/D$  as the angle of attack is increased. It merely gives the relation between  $L/D$  and  $C_L$  for the optimum wing form at a given  $C_L$  value, and for each value of  $C_L$  the wing form will be different (different chord distribution).

**The optimum cruise altitude.**—If cruise at the most efficient lift coefficient  $C_L$  is to be attained, the wing must fly at the altitude where the optimum equilibrium condition

$$W_C = C_L \frac{1}{2} \sigma_C \rho_{st} V_C^2 S \quad (38)$$

is satisfied, since the cruise speed  $V_C$  is specified. (Alternately, of course, the cruise altitude could be specified and the cruise speed calculated. If both the altitude and speed at cruise are specified, the necessary  $C_L$  for cruise is determined and the foregoing procedure gives the maximum value of  $L/D$  at this  $C_L$  value.) The subscript  $C$  denotes the cruise values of the variables and  $\sigma_C$  is the density ratio  $\rho_C/\rho_{st}$ . The density ratio is of course a function of altitude  $h$  and  $\sigma_C = \sigma(h_C)$ . The optimum cruise altitude is then given implicitly by

$$\sigma_C = \frac{W_C}{C_L \frac{1}{2} \rho_{st} V_C^2 S} \quad (39)$$

through the altitude-density function  $\sigma(h)$ . The air density at cruise altitude is

$$\rho_C = \sigma_C \rho_{st} \quad (40)$$

In equation (39),  $W_C$  is the initial cruise weight supported by the wing. In practical aircraft operation with conventionally fueled engines,  $W_C$  will decrease as fuel is used up and if the aircraft is to fly at  $C_L^*$  continuously, the altitude must increase in such degree that

$$\frac{W_C}{\sigma_C} = \text{Constant} \quad (41)$$

**The effective downwash distribution at cruise.**—The effective downwash distribution along the cambered span at cruise must now be determined so that the geometrical twist necessary for optimum loading of the wing can be calculated. The

effective downwash velocity  $w(s)$  is shown in reference 1 to be given by

$$w(s) = w_o \cos \tau(s) \quad (42)$$

In this equation  $w_o$  is the maximum downwash (occurring at the center of the span) and  $\tau$  is the slope of the camber-line tangent at point  $s$ . The effective downwash at a point  $s$  of the camber line is the component of the total induced velocity at point  $s$  normal to the camber line (fig. 8). In the case of symmetrical arc forms the total induced velocity is  $w_o$  and is constant along the arc.

From equation (5)

$$w_o = \frac{\Gamma_o}{N_A \frac{b'}{2}} \quad (43)$$

and if equations (13), (42), and (43) are used with the condition  $W=L$ , it follows that

$$w(s) = \frac{W}{\rho V \left[ \frac{b'}{2} \right]^2 B N_A} \cos \tau(s) \quad (44)$$

Then from the expression for the camber line,  $z(y)$ , there follows

$$\tan \tau = \frac{dz}{dy} \quad (45)$$

whence

$$\cos \tau = \frac{1}{\sqrt{1 + \left[ \frac{dz}{dy} \right]^2}} \quad (46)$$

This equation defines the relation  $\cos \tau$  as a function of the coordinate  $y$ , and since

$$s = \int_0^y \sqrt{1 + \left[ \frac{dz}{dy'} \right]^2} dy' \quad (47)$$

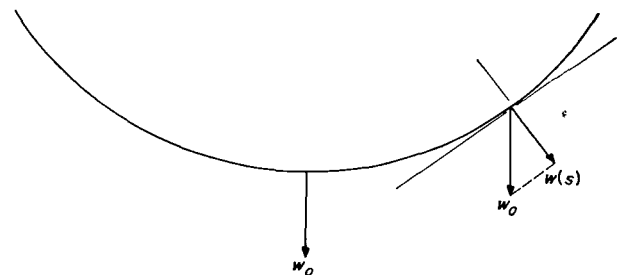


FIGURE 8.—Diagram of induced velocity and its relation to effective downwash.

$\cos \tau$  is also determined as a function of  $s$  (the arc-span coordinate). Thus, the effective downwash distribution corresponding to minimum induced drag becomes known for any flight condition. For the cruise condition, use of equation (44) yields

$$w(s) = \frac{W_c}{\rho_c V_c \left[ \frac{b'}{2} \right]^2 BN_A} \cos \tau(s) \quad (48)$$

**Wing twist function for minimum induced drag.**—The induced angle-of-attack distribution  $\alpha_i(s)$  is defined by

$$\alpha_i(s) = \tan^{-1} \frac{w(s)}{V} \quad (49)$$

where  $w(s)$  is the effective downwash distribution along the arc span. At cruise conditions, substitution of equations (39) and (40) into equation (48) gives

$$\frac{w}{V_c}(s) = \frac{C_L^* S}{2 \left[ \frac{b'}{2} \right]^2 BN_A} \cos \tau(s) \quad (50)$$

The induced angle of attack at cruise is, therefore,

$$\alpha_i(s) = \tan^{-1} \left\{ \frac{C_L^* S}{2 \left[ \frac{b'}{2} \right]^2 BN_A} \cos \tau(s) \right\} \quad (51)$$

This equation can alternately be written as

$$\alpha_i(s) = 2 \frac{C_L^* S}{\pi k [b']^2} \cos \tau(s) \quad (52)$$

by using the usual linearizing assumptions and equation (4).

The required geometrical angle-of-attack distribution  $\alpha(s)$  at cruise is given by

$$\alpha(s) = \alpha_i(s) + \alpha'^* \quad (53)$$

where  $\alpha'^*$  is the section angle of attack corresponding to the optimum section lift coefficient  $c_l = m C_L$ . Under the foregoing assumption of geometrically similar profiles for all sections,  $\alpha'^*$  is of course constant. Substitution of equation (52) into equation (53) gives the geometrical angle of attack (measured as the angle, in the plane normal to the camber line, between the direction of  $V$

and the section chord line) at cruise in terms of the camber and design lift coefficient  $C_L^*$

$$\alpha(s) = \alpha'^* + 2 \frac{C_L^*}{\pi k A} \cos \tau(s) \quad (54)$$

If the geometrical twist function  $\theta(s)$  is defined as

$$\theta(s) = \alpha(s) - \alpha_o \quad (55)$$

where  $\alpha_o$  is the geometrical angle of attack of the root wing section (at  $s=y=0$ ), it can be seen that the twist for an optimum cambered-span wing constructed of similar profiles will be negative, since  $\alpha$  decreases as  $\tau$  increases, as indicated by equation (54). This relationship means that the wing must possess geometrical "washout" for minimum induced drag at cruise.

**Final wing form.**—With the determination of the twist function, all the information necessary for the aerodynamic specification of the total wing form for maximum cruise efficiency is available. The camber line  $z(y)$  specifies the frame upon which the chosen section profiles are to be arranged. For simplicity, the camber line can be assumed to pass through the quarter-chord point of each section or else the location of the profiles relative to the camber line can be specified. The optimum chord distribution  $c(s)$ , as determined by equation (29) when the optimum root chord length is specified, follows directly from the optimization procedure for maximum  $L/D$ . Finally, equation (55) for the twist function specifies the angular arrangement of the section profiles along the camber line, and  $\alpha_o$  gives the geometrical angle of attack of the center wing section.

#### ADDITIONAL DESIGN CONSIDERATIONS

Although the design relations presented have included the principal factors involved in optimizing a wing form for specified operating conditions, several other special factors which are of importance must be considered in a complete wing design. These are briefly discussed in this section.

**Section profile selection.**—A small effective wing area  $S'$  is particularly desirable for cambered wings, especially when use is made of the thick, laminar-flow profiles, such as characterized by the NACA 65<sub>3</sub>-618 wing section. Since the section drag coefficient of such profiles is very small and is essentially independent of the section lift coefficient over a wide lift range (the drag bucket),

use of such profiles operating at a relatively high value of  $c_l$  and with a small chord length can result in a substantial lowering of the wing profile drag at cruise as compared with that of more conventional sections, provided that the full extent of laminar flow can be realized and that the cruise Reynolds number is not so large that the drag bucket has become very narrow. In addition, the relatively large thickness ratio of these airfoils provides considerable depth for housing the wing-spar structure. The attainment of a small value for  $S'$ , however, depends upon the maximum value of  $c_l$  that can be attained for satisfaction of landing or take-off requirements. It thus appears highly desirable when such profiles are used to make full use of such high-lift devices as multiple-slotted flaps in order to increase  $c_{l,L}$  to a value sufficiently high for low-speed operation.

In order to evaluate various wing-section profiles for optimizing the wing  $(L/D)_{max}$  value at cruise conditions, the function

$$\frac{C_L}{C_D} = c_a \frac{C_L}{S'} + \frac{C_L^2}{\pi k A} \quad (56)$$

can be optimized for a series of different profiles, and the profile having the largest value for this parameter can be determined. The final profile selection must of course also be based upon the  $c_{l,max}$  value and upon a sufficient thickness ratio to meet structural requirements.

The optimization considerations are based upon the restrictions that the wing be constructed entirely of similar profiles all operating at the same value of  $c_l$ . It is possible, however, to design the cambered-span wing so that it will possess the maximum possible value of  $L/D$  when the restrictions of operation at constant  $c_l$  and similar profiles are removed. When every section of the wing is simultaneously operating at its own value of  $(L'/D')_{max}$ , the total wing will then have its maximum value of  $L/D$  for a given lift. For example, if the cruise conditions  $W_C$ ,  $V_C$ , and  $h_C$  are specified, the value of  $(L'/D')_{max}$  can be determined for each section by use of the relation

$$\frac{L'}{D'} = \frac{c_l(\alpha') q c c \cos \tau}{D_i' + c_a(\alpha') q c c} \quad (57)$$

where

$$D_i' = \rho_c w \Gamma_C = \frac{1}{2} c_l \frac{W_C}{BN_A \left[ \frac{b'}{2} \right]^2} c \cos \tau \quad (58)$$

and

$$L' = \rho_c V_C \Gamma_C \cos \tau = c_l q c c \cos \tau \quad (59)$$

Under the given cruise conditions, equation (59) leads to the condition

$$c_l c = \text{Constant} \quad (60)$$

for any specific section and use of this condition in equation (57) will ultimately determine the optimum chord length, angle of attack  $\alpha$ , and twist angle for each section, corresponding to the value of  $(L'/D')_{max}$ . The section data used should of course correspond approximately to the anticipated flight Reynolds number of the section.

**Angle-of-attack variations.**—The optimum cambered-span wing is designed primarily for cruise conditions, and the geometrical twist provides the angle-of-attack distribution necessary for the optimum circulation loading at cruise speed. For lower speeds an increase in section angle of attack is necessary if a constant lift is to be maintained. Because of the camber of the span, however, an increase in the effective angle of attack of the center wing sections obtained by pitching the wing will have less effect on the out-board section angles of attack, due to the effect of camber, if the wing is rigid. A possible solution to this problem lies in the use of trailing-edge flaps. By a suitable programing of flap deflection, the section lift coefficient can be varied while maintaining a constant section geometrical angle of attack (corresponding to the cruise condition). In this way, the wing could always operate at essentially the same flight attitude for take-off, landing, and cruise. In addition, it would be possible to maintain an approximately optimum circulation distribution at all flight conditions without need for pitching of the entire wing. The use of such flaps is also quite compatible with the need for high values of  $c_{l,max}$  and small values of  $S'$  at cruise.

**Take-off and landing requirements.**—The design procedure outlined above is based upon the specified landing weight and speed. Inasmuch as the

take-off weight is usually considerably greater than the landing weight, for the same  $c_{l,max}$  the take-off speed must therefore be greater than the landing speed. The take-off speed could be equally well used as the criterion for determining the minimum chord distribution. However, the desirability of maintaining a reasonably small value of  $S'$  for optimum  $L/D$  operation may require some compromise of the minimum landing or take-off speeds, unless means for obtaining very high section lift coefficients, such as external boundary-layer control, are utilized. For special missions where cruise efficiency is critical, use of jet-assisted take-off is quite feasible as a means for overcoming any take-off problems which might exist.

**Structural considerations.**—The preceding design outline has been based solely upon aerodynamic considerations without regard to structural factors. The structural factor of primary importance is the wing structural weight as compared to a flat-span wing producing equal lift. In a complete design analysis, the effects of structural weight must of course be considered. The effect of the span ratio  $\psi$  on weight properties, as well as the possibility of utilizing lightweight aeroelastic wing structures for weight reductions, is discussed in reference 1.

**Special missions.**—In addition to the possibility of using cambered-span wings for improvement of the efficiency of conventional aircraft, there are a number of special areas where application of such wings may be of significant value. Since the primary advantage of cambered wings lies in their high effective aspect ratios for a given span length, operational missions where high induced drag is a serious problem are of particular interest. There are several such missions. In the operation of STOL aircraft, the very low take-off and landing speeds require operation at very high  $C_L$  values with very high  $D_i$ . For such airplanes, operating conditions often severely limit the allowable span length and hence the geometrical aspect ratio. In addition to the very high induced drag encountered by such aircraft, it is predicted in reference 2 that at very large values of  $C_L$  (or for small values of  $A$ ), the airfoil lift can be appreciably reduced by the large downwash velocities. Use of spanwise camber could help in alleviating both problems. In situations where the physical span length is limited, camber can be used to

increase the effective value of the aspect ratio over that of flat-span wings. Various other areas include efficient subsonic cruise at extremely high altitudes (where the low density requires high  $C_L$  values), high endurance aircraft, and cargo aircraft operation with increased payload. Possible stability and control applications are also suggested in reference 1.

#### ILLUSTRATIVE DESIGN OF A CAMBERED-SPAN WING

In order to illustrate briefly the application of the foregoing design procedure, calculations have been carried out for a cambered-span wing which satisfies an arbitrary set of prescribed operating conditions. The conditions selected are typical of current operational requirements met by conventional-winged transport aircraft. No attempt has been made in this illustration to determine the absolute optimum wing form as regards  $(L/D)_{max}$ , and the wing chord distribution used corresponds to the minimum value as set by the prescribed landing condition. The wing section chosen for the illustration is the NACA 65<sub>3</sub>-618 profile. However, the use of laminar-flow profiles is in no way mandatory with cambered wings, although such profiles possess some advantages because of their low drag coefficients. It is assumed for purposes of illustration that the section profile-drag coefficients obtained in wind-tunnel tests can be realized in full-scale, practical operation. In reality, extremely smooth wing surfaces would of course be required for extensive areas of laminar flow. The results of this study, therefore, may be considered as a realistic, although not conservative, indication of the general level of aerodynamic efficiency of the particular cambered wing for the given operating requirements.

It should perhaps be emphasized that the relative efficiencies of the flat and cambered wings of this illustration are valid only for the particular set of operating conditions imposed. The particular camber line used was quite arbitrary and use of a more optimum camber form might result in significant increases in wing efficiency. In any specific application, the most optimum camber form can only be found by a series of design trials based upon the particular operational requirements.

**BASIC DESIGN CONDITIONS**

The cambered wing arbitrarily chosen for this illustration has a circular-arc camber line with  $\beta=0.8$  and  $\frac{b'}{2}=58$  feet. Thus, when optimally loaded, the wing will have the following values for its constants:  $k=1.32$ ,  $N_A=2.561$ , and  $B=1.619$ , as shown in figures 4 and 6. The basic flat wing chosen for comparison purposes and as a basis for coefficients, has the following characteristics: elliptical planform,  $\frac{b}{2}=58$  feet,  $A=8$ ,  $S=1,683$  square feet, and the wing section is the NACA 65<sub>3</sub>-618 throughout. This same profile is used for the cambered wing.

The prescribed speed and weight conditions are

$$\left. \begin{aligned} W_L &= 85,000 \text{ lb} & W_C &= 110,000 \text{ lb} \\ V_L &= 105 \text{ mph} & V_C &= 310 \text{ mph} \end{aligned} \right\} \quad (61)$$

These operating requirements and the span and wing area of the flat reference wing are typical of the operating specifications of an actual transport aircraft wing.

**THE SPANWISE CAMBER-LINE GEOMETRY**

The equation of a circular-arc spanwise camber line is given by

$$\begin{aligned} z &= r - [r^2 - y^2]^{1/2} \\ &= r[1 - \cos \tau] \quad \left( -\frac{b'}{2} \leq y \leq \frac{b'}{2} \right) \end{aligned} \quad (62)$$

where  $r$  is the radius of curvature of the arc. (See fig. 9.) For any values of  $\beta$  and semispan  $b'/2$ ,

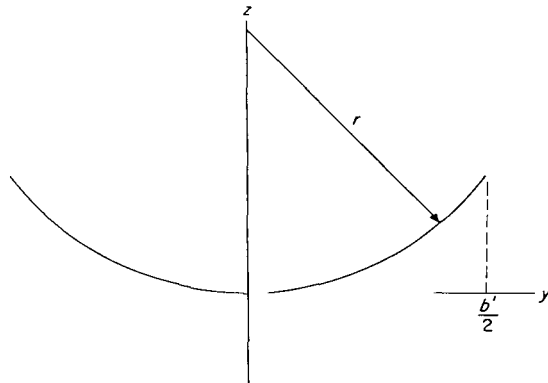


FIGURE 9.—Geometry of a circular-arc camber line.

the value of  $r$  is given by

$$r = \frac{1}{2} \frac{b'}{2} \frac{1 + \beta^2}{\beta} \quad (63)$$

and substitution of equation (63) into equation (62) gives the dimensional camber line  $z(y)$ . For the present configuration where  $\beta=0.8$  and  $\frac{b'}{2}=58$  feet, the function  $z(y)$  is as shown in figure 10.

Since most of the wing design variables are expressed as functions of arc length  $s$  instead of  $y$  (fig. 2), the relation  $s(y)$  is needed. This function is obtained by use of the arc-length expression

$$s = \int_0^y \sqrt{1 + \left[ \frac{dz}{dy'} \right]^2} dy' = r\tau \quad (64)$$

which, when applied to equation (62), yields

$$s(y) = r \sin^{-1} \frac{y}{r} \quad (65)$$

Equation (65), when plotted for the present case, gives the curve shown in figure 11. This curve allows direct conversion from one system of coordinates to the other.

It is also necessary to determine the function  $\cos \tau(s)$ . The relation for  $\tau(y)$  is given by

$$\begin{aligned} \tau(y) &= \tan^{-1} \frac{dz}{dy} \\ &= \tan^{-1} \frac{y}{\sqrt{r^2 - y^2}} \\ &= \sin^{-1} \frac{y}{r} \end{aligned} \quad (66)$$

where  $r$  is given by equation (63). Use of equation (65) allows the determination of  $\tau(s)$ , and the function  $\cos \tau(s)$  follows directly. Alternately,

$$\begin{aligned} \cos \tau(y) &= \frac{1}{\sqrt{1 + y^2(r^2 - y^2)^{-1}}} \\ &= \sqrt{1 - \frac{y^2}{r^2}} \end{aligned} \quad (67)$$

The function  $\cos \tau(s)$  for the present camber line is plotted in figure 12.

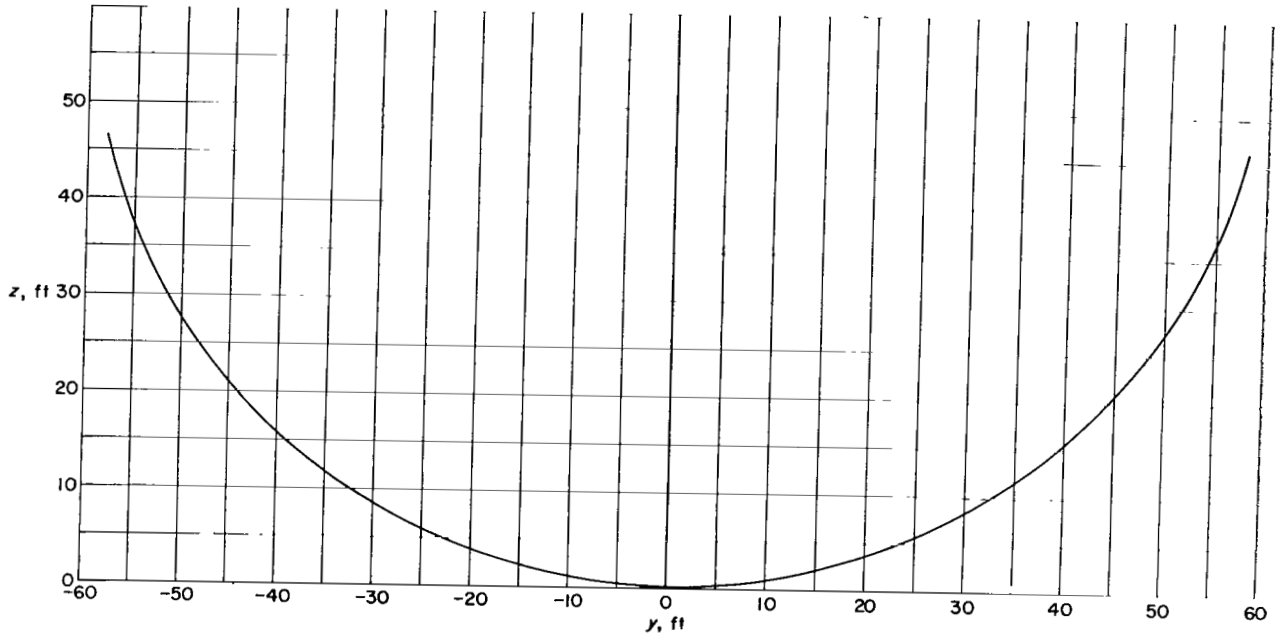


FIGURE 10.—Circular-arc camber line used in the illustrative calculations.  $\beta=0.8$ ,  $\frac{b'}{2}=58$  feet.

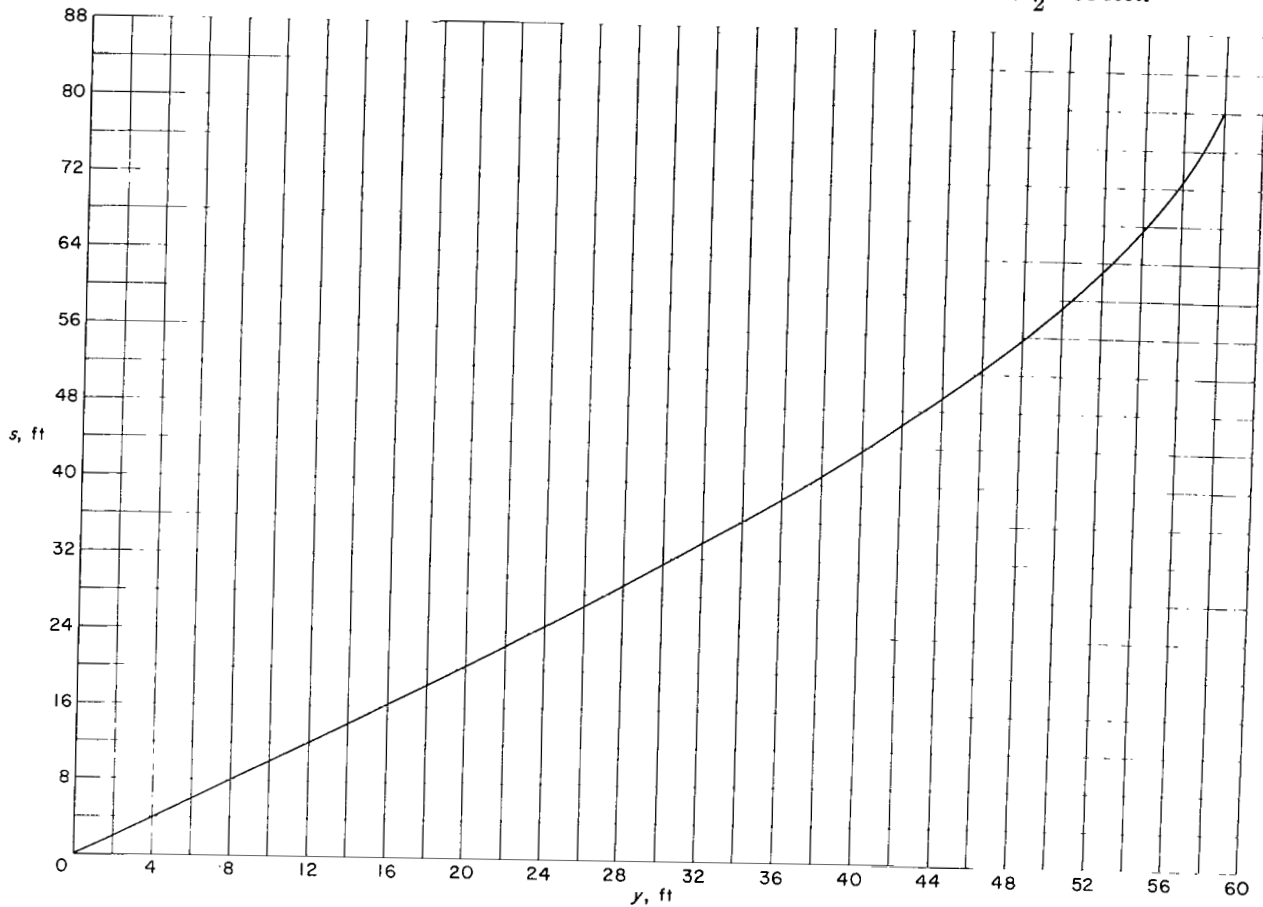


FIGURE 11.—Relation between arc length coordinate  $s$  and span coordinate  $y$  for a circular-arc camber line of  $\beta=0.8$ .

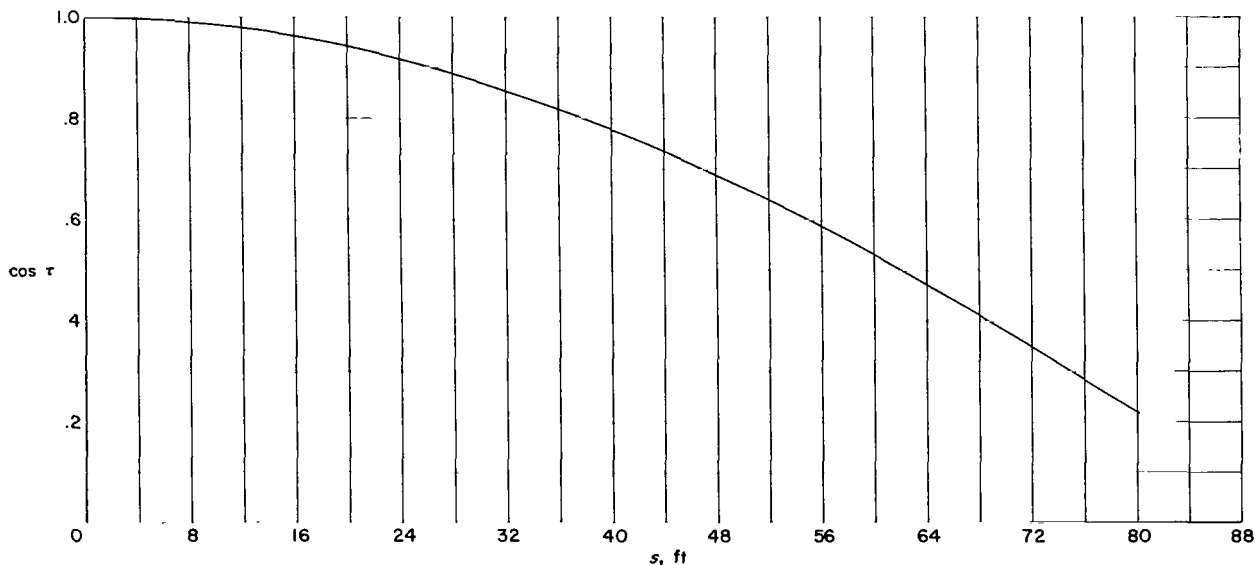


FIGURE 12.—Variation of  $\cos \tau$  with arc length for a circular-arc camber line of  $\beta=0.8$ .

**THE CHORD FUNCTION  $c(s)$**

Although the foregoing procedures allow the optimum chord distribution to be determined for the cambered-span wing, the chord distribution to be used for the purposes of this example corresponds to that set by the landing requirements listed previously. Thus, the chord distribution used is not necessarily optimum.

The chord function is obtained by substitution of the landing conditions of equation (61) into equation (18), with  $\rho_L$  taken as 0.002378 slug

per cubic foot. The function  $\frac{\Gamma}{\Gamma_0}(s)$  is given indirectly in figure 4 as  $\frac{\Gamma}{\Gamma_0}(\gamma)$ , and it is assumed

that by use of a suitable slotted-flap arrangement the value  $c_{i,L}=3.0$  is operationally attainable with the NACA 65<sub>3</sub>-618 profile. Values of  $c_{i,L}$  as high as 3.2 are obtainable with double slotted flaps (see ref. 3), and the chosen value of 3.0 is not unusually optimistic, even without the use of synthetic means of boundary-layer control. The resulting chord distribution  $c(s)$  is shown in figure 13.

**THE WING DRAG POLAR FOR MINIMUM INDUCED DRAG**

Use of equation (19) yields the effective physical area of the wing  $S'$  as 1,340 square feet. Equation (27) gives the value of  $m$  as 1.675, and the relation between total and section lift coefficient becomes

$$c_l = 1.675 C_L \quad (68)$$

Thus, in conjunction with the section drag polar for the NACA 65<sub>3</sub>-618 section (see fig. 14), the wing drag function  $C_D(C_L)$  follows directly from equation (28). The "polar" for the present wing series is presented in figure 15, where the function  $\frac{L}{D}(C_L)$  is also plotted. From this latter curve the value of  $C_L$  for maximum  $L/D$  is

$$C_L^* = 0.315 \quad (69)$$

The polar of figure 14(a) is for a Reynolds number of  $9 \times 10^6$ , while the cruise flight Reynolds number (based on the wing root chord) is approximately  $27 \times 10^6$ . Although experimental data on the NACA 65<sub>3</sub>-618 section does not exist for Reynolds numbers above  $9 \times 10^6$ , there is evidence that similar profiles operating at the design  $c_l$  value of 0.528 have even lower values of the drag coefficient for Reynolds numbers up to  $35 \times 10^6$ . (See ref. 4, fig. 14, p. 18.) With increasing Reynolds numbers above  $9 \times 10^6$ , however, the extent of the low-drag bucket decreases slowly and for high values of  $c_l$  ( $c_l > 0.8$ ) the drag coefficient (for sections near the wing root) will probably be slightly greater than shown in figure 14(a). Still, since most of the wing will be operating at local Reynolds numbers considerably below  $27 \times 10^6$ , where the section drag coefficient is actually lower than indicated in figure 14(a), the total wing drag coefficient variation should be very close to that based on figure 14(a).

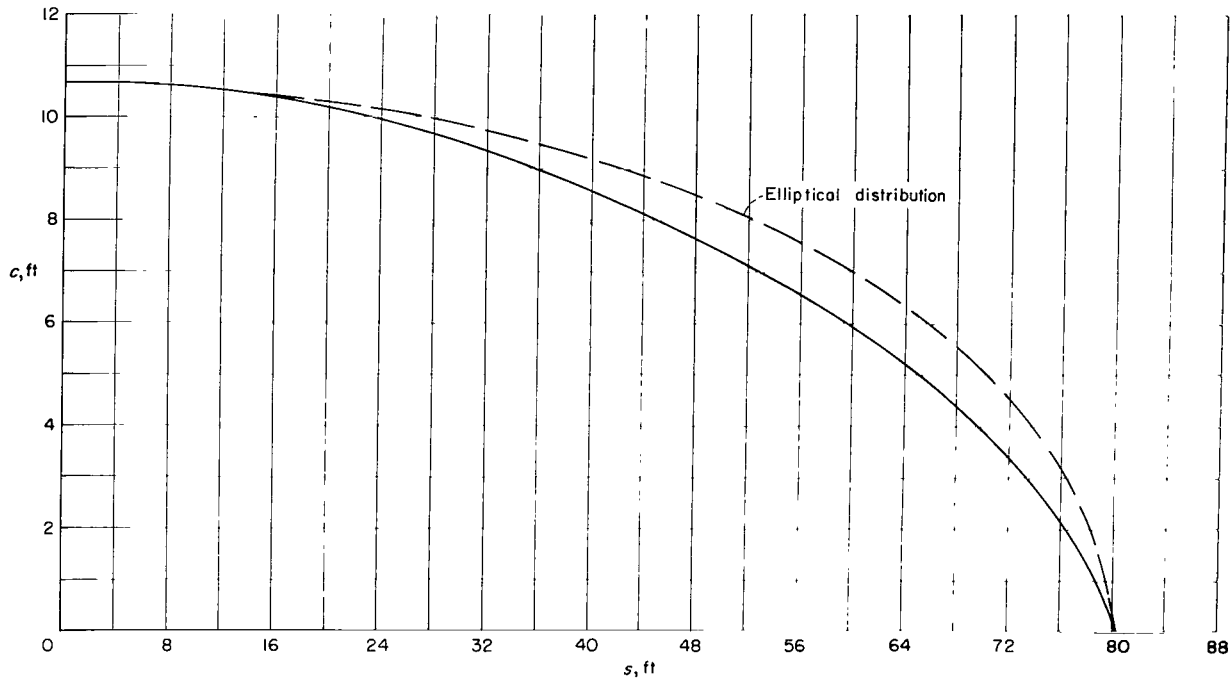
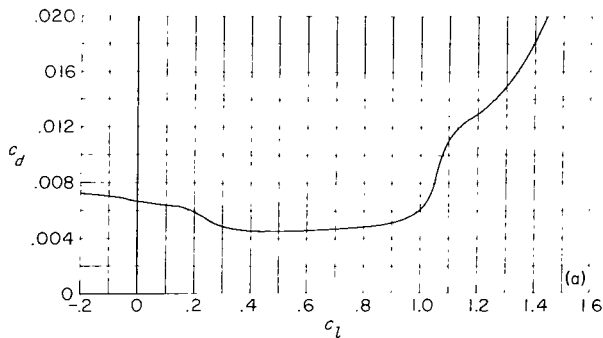
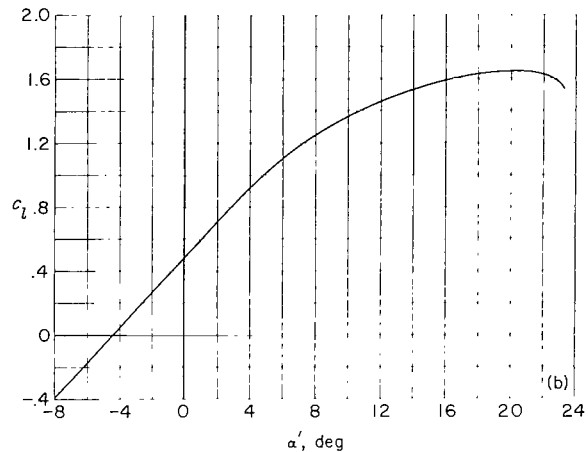


FIGURE 13.—Minimum-chord-length distribution for circular-arc wing.  $\beta=0.8$ .



(a) Drag polar.

FIGURE 14.—Section coefficients for the NACA 65<sub>3</sub>-618 profile.



(b) Lift curve.

FIGURE 14.—Continued.

**THE OPTIMUM CRUISE ALTITUDE**

From equations (39) and (69) there follows

$$\sigma_c = 0.845 \quad (70)$$

whence

$$h_c = 5,600 \text{ ft} \quad (71)$$

At this altitude, the Mach number for cruising flight is 0.416, which is considerably below the critical value at the section operational lift coefficient (see fig. 14(c)).

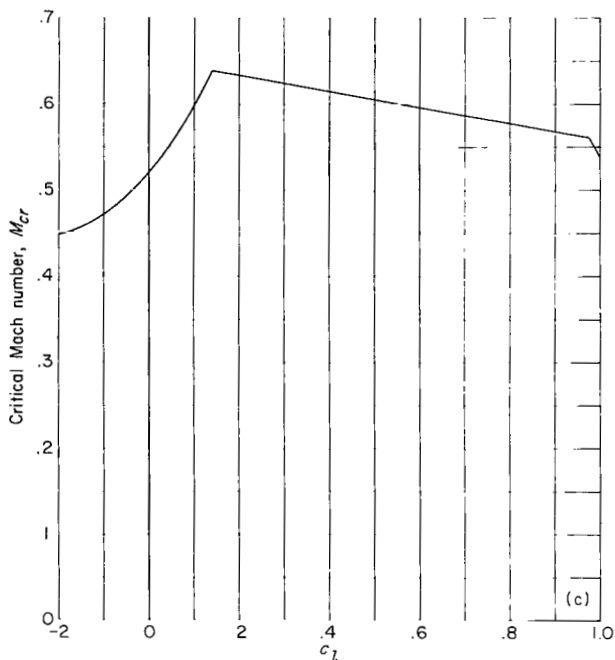
**THE EFFECTIVE DOWNWASH AT CRUISE**

From equation (50) and figure 12 the downwash distribution  $w(s)$  may be determined, and by use

of either of equations (49) or (52) the induced angle-of-attack distribution may be calculated. These two functions are presented in figure 16, for the present wing.

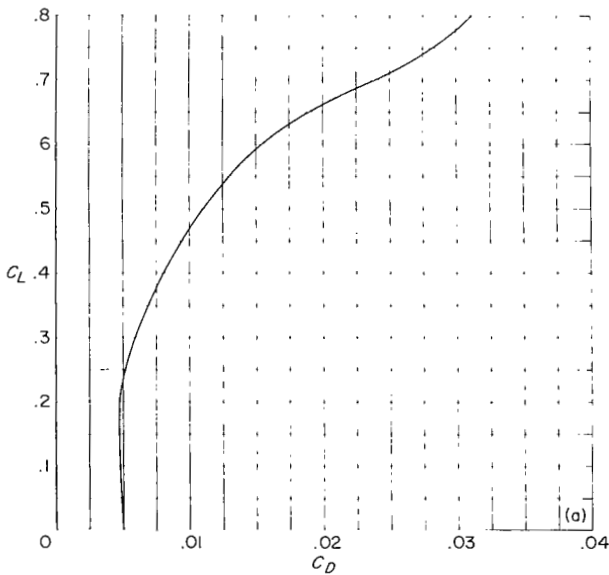
**THE TWIST FUNCTION  $\theta(s)$**

The value of  $\alpha'^*$  (eq. (53)), corresponding to the optimum section force coefficient  $c_l = m(C_L^* = 0.528)$ , is obtained from the section lift curve shown in figure 14(b) and equals  $0.4^\circ$ . Equations (53) and (55) can be used to calculate the wing geometrical angle-of-attack and twist distributions



(c) Critical Mach number.

FIGURE 14.—Concluded.



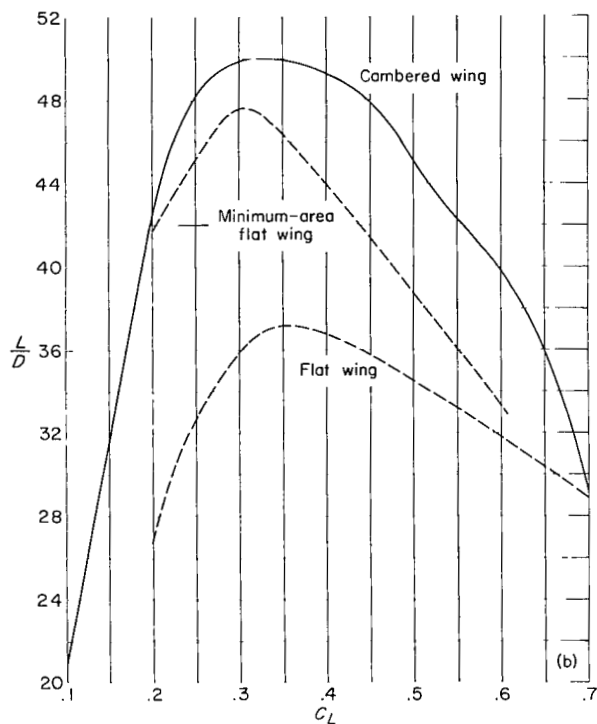
(a) Drag polar.

FIGURE 15.—Total drag polar and  $L/D$  variation for the cambered wing.

$\alpha(s)$  and  $\theta(s)$ . These functions are plotted in figure 17 for the example wing.

**THE FINAL WING FORM**

The relations shown graphically in figures 10, 13, and 17, together with the specification of the



(b)  $L/D$  variation.

FIGURE 15.—Concluded.

NACA 65<sub>3</sub>-618 section, fully determine the physical form of the wing for cruise at the maximum value of  $L/D$  (for the particular chord function being used). As can be seen from figure 13, the variation of the chord length along the arc span is different from an elliptical distribution, especially along the outer 60 percent of the arc span. From figure 17 it is seen that the operational angles of attack at cruise are very small, due primarily to the high amount of camber of the basic section. Only a very slight amount of washout is required, the total twist amounting to only  $-0.85^\circ$ .

The  $L/D$  variation of the flat reference wing is plotted in figure 15(b), where the maximum value is seen to be 37.2 at a lift coefficient of approximately 0.35. The degree to which the efficiency of the flat wing can be improved is indicated in this same figure by the curve labeled "Minimum-area flat wing." This  $L/D$  variation is for a flat-span wing which possesses a minimum chord distribution based upon the same operational conditions as the cambered-span wing. This minimum-area flat wing is assumed to have a proper twist distribution so that minimum

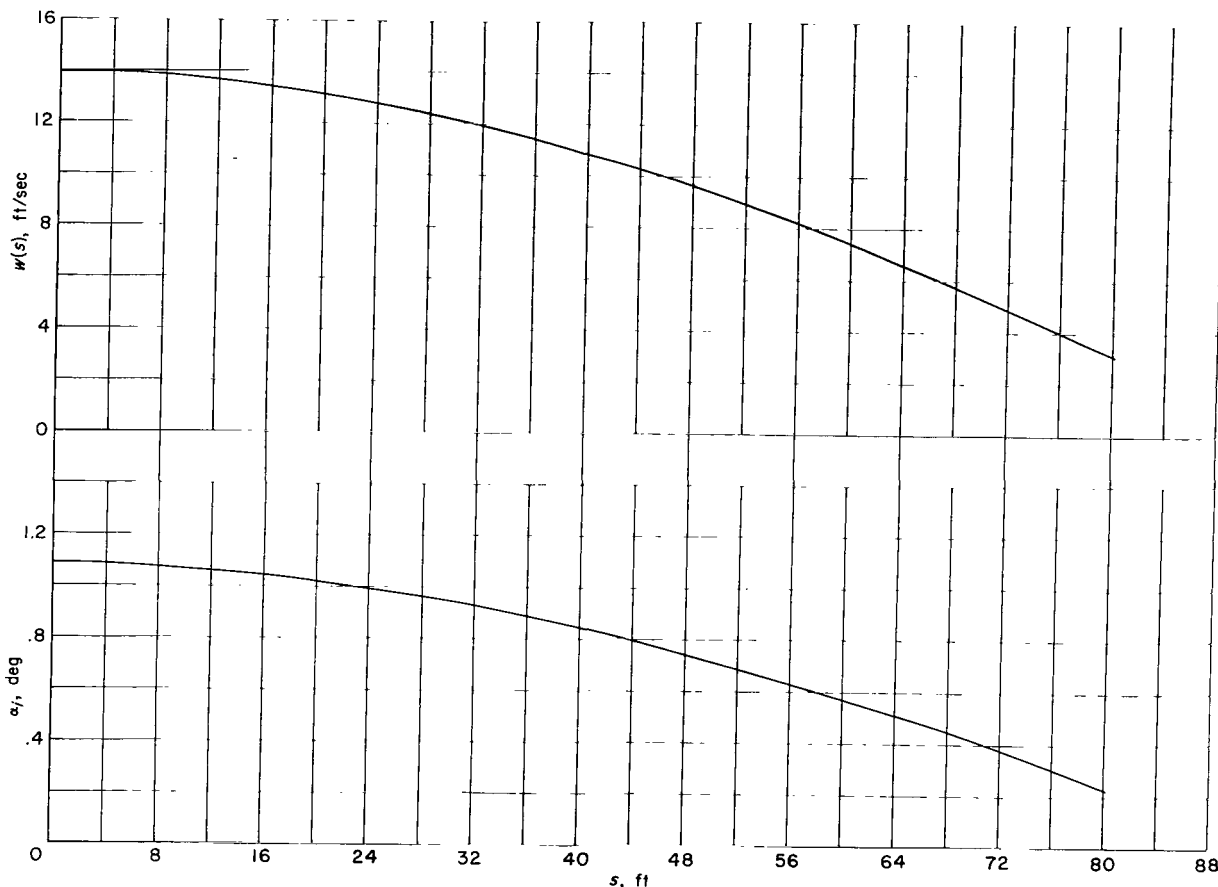


FIGURE 16.—Downwash and induced angle-of-attack distributions for the cambered wing.

induced drag is obtained. The effective area of this wing is only 1,000 square feet. It is evident that appreciable decreases in the profile drag are theoretically possible when the physical wing area is reduced.

The  $L/D$  variation for the cambered-span wing is shown as the top curve in figure 15(b), where it is seen that a maximum value of 50.0 occurs at  $C_L=0.315$ . The cambered-span wing (at least for the conditions and assumptions of this example) is more efficient than either the reference or minimum-area flat wings for a given lift. Although the profile drag is a significant part of the total drag at the value of  $C_L$  for  $(L/D)_{max}$  that occurs in this particular example, it is of much less importance at the higher values of  $C_L$  where the induced drag predominates.

All the comparisons cited are based on the use of the NACA 65<sub>3</sub>-618 airfoil section and merely indicate the relative efficiencies of a specific cambered-span wing (circular arc,  $\beta=0.8$ ) and a specific flat-span wing under a particular set of specified

operating conditions. Neither of these wings can be said to possess maximum efficiency in the sense of absolute values obtainable. It is possible that by use of other airfoil sections and other spanwise-camber forms, and with more optimum chord-length distributions, even higher efficiencies could be obtained with both the flat and cambered-span wings.

An additional point of interest in figure 15(b) is the value of  $L/D$  for  $C_L$  values greater than  $C_L^*$ . Even when wings are designed for operation at  $C_L$  values considerably above  $C_L^*$ , the  $L/D$  of the cambered-span wing is still considerably greater than the  $(L/D)_{max}$  of the flat-span wing, at least for the assumed conditions of this specific example. This difference means that with the specified value of  $W_c$ , the cambered wing could cruise much more efficiently at high altitudes than could the flat wing. As  $C_L$  increases beyond 0.7, however, the cambered wing becomes less efficient than the basic flat wing. This efficiency loss, of course, is purely

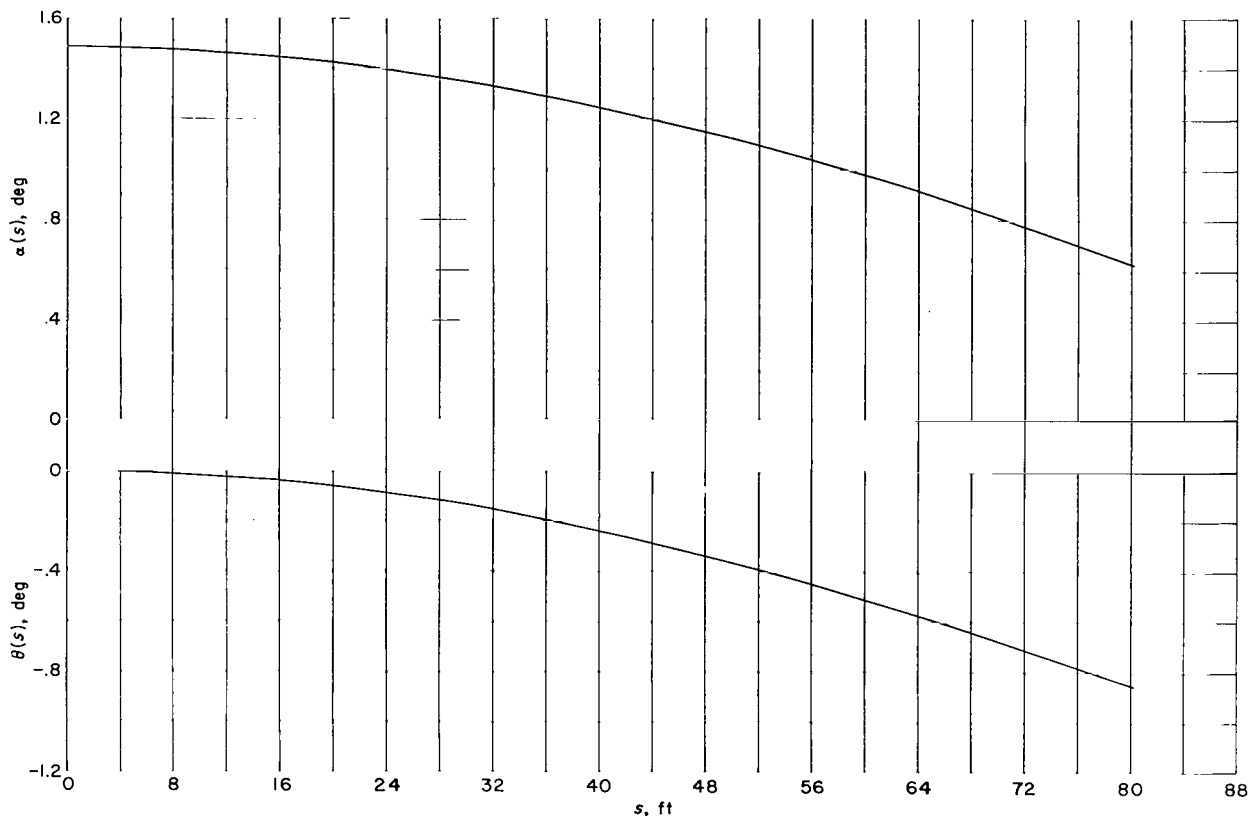


FIGURE 17.—Geometrical angle-of-attack and twist distributions for the cambered wing.

the consequence of the relatively small section chord length of the cambered-span wing, resulting from the completely arbitrary choice of a minimum chord length to satisfy the landing conditions. This chord distribution may in no way be the optimum distribution for large  $C_L$  values. At high values of  $C_L$  the sectional operational lift coefficient  $c_l = mC_L$  exceeds the extent of the laminar flow capabilities of the particular section being used, and the profile drag becomes exceedingly large (on the same order of or larger than the induced drag). For flight at high  $C_L$  values the cambered-wing profile drag can be considerably lowered by increasing the section chord length to its optimum value, by means of the optimization procedure previously outlined. This procedure of course would also aid in reducing the value of  $c_{l,max}$  required for landing.

#### DETERMINATION OF THE WING PITCHING MOMENT

The pitching-moment equation for the most general case of a wing composed of an arbitrary

development of section profiles, each operating with its optimum value of  $c_l$  and chord length  $c$  is considered first. Then the equation for the special case of a wing which is constructed of similar profiles throughout, with each section operating at the same  $c_l$  value, is derived. It is assumed in both of these cases that corresponding values of the functions  $c_l(s)$ ,  $c_d(s)$ ,  $c_{di}(s)$ ,  $c_{m,c/4}(s)$ ,  $c(s)$ , and  $w(s)$  have been determined by the foregoing methods and that the corresponding flight dynamic pressure at cruise,  $\frac{1}{2}\rho V^2$ , is also known. The value of  $c_{m,c/4}$  is, of course, determined from the section pitching-moment curve  $c_{m,c/4}(c_l)$  for the  $c_l$  value at which the section is operating.

The equations are developed for two pitch-axis locations. The first location is for the  $Y$ -axis of the wing camber line and the second is for an arbitrary axis location. The derivations that follow are based upon the assumption that both types of wings are so constructed that the camber line  $z(y)$  passes through the quarter-chord point of the section profiles. For wings which are not constructed in this manner, proper account must

be taken of the displacement distance of the local profile quarter-chord point from the spanwise camber line.

**PITCHING MOMENT OF THE MOST GENERAL WING FORM**

**The section pitching-moment contribution.**— Consider first the section with the quarter-chord point located at the point  $(y, z)$  on the span line of a cambered-span wing. This profile lies in a plane which is normal to the camber line at  $(y, z)$  and thus makes an angle  $\tau$  with the vertical, where  $\tau$  is the slope of the tangent line at the point. (See fig. 7.) At the design operating conditions the section will produce a pitching moment of intensity  $M_{c/4}'$  about the spanwise camber line. This moment is a function of  $c_l$ , the operating force coefficient of the section, where

$$c_l = \frac{F'}{\frac{1}{2}\rho V^2 c} \quad (72)$$

The component of this moment about an axis through the quarter-chord point and parallel to the  $Y$ -axis of the camber line is  $M_{c/4}' \cos \tau$ . The force system creating this moment is shown in figure 18 for the particular case where the section chord is alined with the direction of the free-stream flow. For the coordinate system shown in this figure with the origin at the center of the camber line, the section pitching moment about the horizontal axis through the quarter-chord point is

$$M_{c/4}' \cos \tau = -L'x + D_o'[z' - z] \quad (73)$$

where  $L' = F' \cos \tau$  and  $z'$  is the distance of the

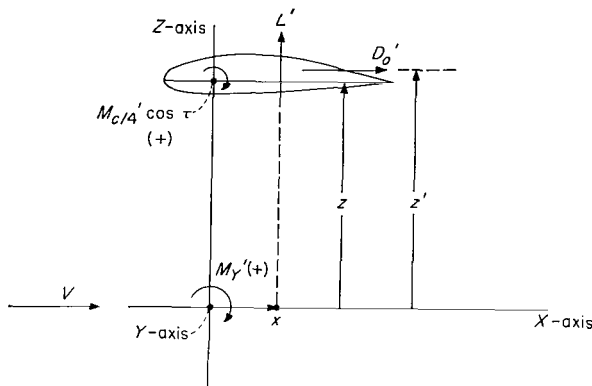


FIGURE 18.—Force and moment system for a wing section at an arbitrary spanwise location.

line-of-action of  $D_o'$  above the  $Y$ -axis, being positive in the upward direction. The positive direction of the resulting pitching moment is as shown in figure 18. The pitching moment of this section about the  $Y$ -axis of the airfoil is given by

$$M_{Y'}' = -L'x + D_o'z' + D_i'z \quad (74)$$

and since

$$D_o'z' = D_o'[z' - z + z] \quad (75)$$

the moment becomes

$$M_{Y'}' = M_{c/4}' \cos \tau + D'z \quad (76)$$

Consider now the case where the pitch axis is located at any arbitrary position having coordinates with respect to the  $Y$ -axis of the camber line  $x_P$  and  $z_P$ , as shown in figure 19. The section moment about this axis is

$$\begin{aligned} M_{P'}' &= -L'[x - x_P] + D_o'[z' - z_P] + D_i'[z - z_P] \\ &= -L'x + D_o'[z' - z] + L'x_P + D'[z - z_P] \\ &= M_{c/4}' \cos \tau + L'x_P + D'[z - z_P] \end{aligned} \quad (77)$$

The subscript  $P$  denotes the arbitrary axis position and  $z_P$  is defined as positive when the pitch axis lies above the  $Y$ -axis of the airfoil.

When the section force coefficient  $c_l(s)$  (eq. (72)) is specified, along with the chord function  $c(s)$ , the pitching moment of each section can be determined for either of the axis locations

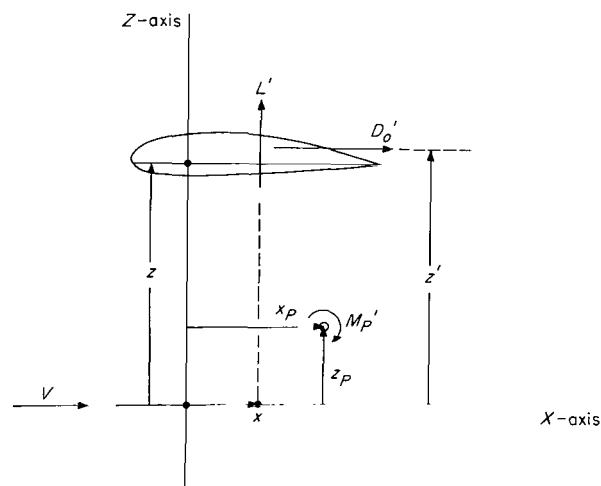


FIGURE 19.—Moment relations for an arbitrary axis location.

of equations (76) or (77) since

$$M_{c/A}'(s) = c_{m,c/A}(s) \frac{1}{2} \rho V^2 c(s)^2 \quad (78)$$

The section moment, moment coefficient, and chord-length distributions are continuous functions of the arc-length coordinate  $s$ .

**Wing pitching moment about  $Y$ -axis.**—The total pitching moment of the wing, with regard to the  $Y$ -axis, is obtained by integrating the contributions of the sections along the arc span,

$$M_Y = \int_{-s_t}^{s_t} M_Y' ds \quad (79)$$

and substitution of  $M_Y'$  from equation (76) yields

$$M_Y = \int_{-s_t}^{s_t} [M_{c/A}' \cos \tau + D' z] ds \quad (80)$$

In this equation the factors are all functions of  $s$ . The moment  $M_{c/A}'$  is given by equation (78), where  $c_{m,c/A}$  is a function of the sectional force coefficient  $c_t$ . The drag force  $D'$  is made up of two components, the profile drag  $D_o'$  and the local induced drag  $D_i'$  where

$$D_o' = c_d q c \quad (81)$$

and

$$D_i' = F' \tan \alpha_i \quad (82)$$

As has been shown previously

$$F' = c_l q c \quad (83)$$

and

$$\tan \alpha_i = \frac{w}{V} \quad (84)$$

where  $w$  is the induced velocity component normal to the lifting line (the "effective" downwash, as given by eq. (42)).

Thus, equation (80) can be written in the expanded form

$$M_Y = q \int_{-s_t}^{s_t} \left\{ c_{m,c/A} c^2 \cos \tau + z \left[ c_d c + c_l \frac{w}{V} c \right] \right\} ds \quad (85)$$

The function  $\cos \tau(s)$  can be determined as a function of  $y$  from the geometry of the camber

line  $z(y)$ ,

$$\cos \tau = \frac{1}{\sqrt{1 + \left[ \frac{dz}{dy} \right]^2}} \quad (86)$$

and then as a function of  $s$  from the relation

$$s = \int_0^y \sqrt{1 + \left[ \frac{dz}{dy'} \right]^2} dy' \quad (87)$$

From equation (87),  $z$  can also be determined as a function of  $s$ . Since all factors of the integrand of equation (85) are variables in the general case being considered, this integral cannot be further simplified.

**Wing moment about arbitrary axis.**—The wing pitching moment  $M_P$  about an arbitrary axis  $P(x_P, z_P)$  follows directly by substitution of equation (77) into the integral

$$M_P = \int_{-s_t}^{s_t} M_P' ds \quad (88)$$

Thus,

$$M_P = q \int_{-s_t}^{s_t} \left\{ c_{m,c/A} c^2 \cos \tau + \left[ c_d c + c_l \frac{w}{V} c \right] z + x_P c_l c \cos \tau - \left[ c_d c + c_l \frac{w}{V} c \right] z_P \right\} ds \quad (89)$$

Alternately, equation (89) can be written as

$$M_P = M_Y + q x_P \int_{-s_t}^{s_t} c_l c \cos \tau ds - q z_P \int_{-s_t}^{s_t} \left[ c_d + c_l \frac{w}{V} \right] c ds \quad (90)$$

#### PITCHING MOMENT OF A WING CONSTRUCTED OF SIMILAR PROFILES

The pitching-moment relations for a cambered-span wing which is constructed entirely of similar profiles, all operating at the same value of the section force coefficient  $c_l$  can now be derived.

**Wing pitching moment about  $Y$ -axis.**—The pitching moment about the  $Y$ -axis of a wing with similar airfoil sections along the span can be obtained directly by specializing the general form of equation (85). Under the design restrictions, it follows that the chord distribution  $c(s)$  can be

written as

$$c(s) = c_o \frac{\Gamma}{\Gamma_o} \quad (91)$$

where  $c_o$  is the wing root chord and  $\Gamma/\Gamma_o$  is the nondimensional circulation distribution for minimum induced drag. Thus, equation (85) becomes

$$M_Y = qc_o \left[ c_o c_m c_l \int_{-s_t}^{s_t} \left( \frac{\Gamma}{\Gamma_o} \right)^2 \cos \tau ds + c_d \int_{-s_t}^{s_t} \frac{\Gamma}{\Gamma_o} z ds + c_l \int_{-s_t}^{s_t} \frac{\Gamma}{\Gamma_o} \frac{w}{V} z ds \right] \quad (92)$$

**Pitching moment about an arbitrary axis.**—The pitching moment about an arbitrary axis  $P$  is obtained directly by specializing equation (90),

$$M_P = M_Y + qc_o \left[ c_l x_P \int_{-s_t}^{s_t} \frac{\Gamma}{\Gamma_o} \cos \tau ds - c_d z_P \int_{-s_t}^{s_t} \frac{\Gamma}{\Gamma_o} ds - c_l z_P \int_{-s_t}^{s_t} \frac{\Gamma}{\Gamma_o} \frac{w}{V} ds \right] \quad (93)$$

Since the following relations are valid:

$$\int_{-s_t}^{s_t} \frac{\Gamma}{\Gamma_o} ds = \frac{b'}{2} G \quad (94)$$

$$\frac{w}{V} = \frac{w_o}{V} \cos \tau \quad (95)$$

$$\int_{-s_t}^{s_t} \frac{\Gamma}{\Gamma_o} \frac{w}{V} ds = \frac{w_o}{V} \int_{-s_t}^{s_t} \frac{\Gamma}{\Gamma_o} \cos \tau ds = \frac{b'}{2} \frac{w_o}{V} B \quad (96)$$

equation (93) becomes

$$M_P = M_Y + qc_o \left[ \frac{b'}{2} c_l B x_P + \frac{b'}{2} c_d G z_P + \frac{b'}{2} \frac{w_o}{V} c_l B z_P \right] \quad (97)$$

Here, the moment  $M_Y$  of course applies to the case of the similar-section wing, as given by equation (92).

**VARIATION OF  $C_{m,P}$  WITH  $C_L$  FOR GENERAL WING FORM**

Equation (90), in conjunction with equation (85), gives the wing pitching moment  $M_P$  about any arbitrary axis. In order to express this equation in dimensionless form, a pitching-

moment coefficient can be defined on the basis of the wing area  $S$  and mean aerodynamic chord  $\bar{c}$  of a flat-span reference wing

$$C_{m,P} = \frac{M_P}{\frac{1}{2} \rho V^2 S \bar{c}} \quad (98)$$

The lift of the cambered-span wing can also be expressed in coefficient form

$$C_L = \frac{L}{\frac{1}{2} \rho V^2 S} \quad (99)$$

and since  $C_L$  is related to the section force-coefficient distribution  $c_l(s)$  and chord distribution  $c(s)$  by

$$C_L = S^{-1} \int_{-s_t}^{s_t} c_l c \cos \tau ds \quad (100)$$

the variation of  $M_P$  and hence  $C_{m,P}$  with  $C_L$  can be determined.

It should perhaps be emphasized that the function  $C_{m,P}(C_L)$  does not represent the variation of  $C_{m,P}$  as the angle of attack of a particular wing is varied, as with conventional airfoils. Rather, it gives the pitching-moment-coefficient variation with the optimum wing form corresponding to the maximum wing  $L/D$  at each value of  $C_L$ . That is, the physical wing form is different for each value of  $C_L$ .

**VARIATION OF  $C_m$  WITH  $C_L$  FOR SIMILAR-PROFILE WING**

The pitching-moment coefficient of the wing constructed of similar section profiles all operating at the same value of  $c_l$  is also given by equation (98), but with the value of  $M_P$  being obtained from equation (97). In this special case, however, equation (100) reduces to the simple form

$$C_L = \frac{c_l}{m} \quad (101)$$

where  $m$  is a constant (eq. (27)). Thus, the individual terms of equation (97) can be directly evaluated for each value of  $C_L$ , using the corresponding section force coefficient  $c_l = m C_L$ .

**LOCUS OF TRIM AXIS**

As can be seen from equation (90) for the most general form of the pitching moment, there are an infinite number of axis locations for which  $M_P$  will be equal to zero. An axis for which

$M_P=0$  will be defined as a trim axis. A knowledge of the locus of such axes is obviously important for determining aircraft component arrangements which will possess satisfactory trim properties at cruise flight conditions.

For a given set of cruise flight requirements and the corresponding optimum wing form, the value of  $M_Y$  (eq. (90)) can be calculated and the values of the two integral factors determined. Then, the trim condition  $M_P=0$  leads to the equation

$$z_T = \frac{M_Y + x_T q \int_{-s_t}^{s_t} c_l c \cos \tau ds}{q \int_{-s_t}^{s_t} \left[ c_d + c_l \frac{w}{V} \right] cds} \quad (102)$$

which defines the locus of the trim axis,  $z_T = z_T(x_T)$ . Since  $M_Y$  and the integrals are constants in this equation, the  $z_T$  value for any  $x_T$  location is thus determined for the trim condition.

For the case of a wing constructed of similar profiles operating at the same value of  $c_l$ , the locus  $z_T = z_T(x_T)$  is obtained from equation (97),

$$z_T = \frac{M_Y + \left[ qc_o c_l B \frac{b'}{2} \right] x_T}{qc_o \left[ c_d G \frac{b'}{2} + \frac{w_o}{V} c_l B \frac{b'}{2} \right]} \quad (103)$$

By use of the equations developed herein, the wing pitching moment of any optimally loaded cambered-span airfoil can be calculated for the design flight condition. In the general case, the optimum nondimensional circulation loading  $\Gamma/\Gamma_o$  may have to be determined by the electrical analog method and hence must be expressed in graphical form. Consequently, the ensuing design analysis and moment determinations will also have to be carried out graphically. Even in the particular cases where  $\Gamma/\Gamma_o$  can be obtained analytically by conformal transformations, the resulting functions may result in extremely complex integrals, so that machine solutions are necessary.

In the particular case of the similar-profile wing, the calculation of the pitching-moment variation with lift coefficient is considerably simplified because most of the integrals are then constants.

The locus equations (102) and (103) can be used to determine the proper location of the

center of gravity of a complete aircraft configuration so as to optimize the longitudinal trim requirements at cruise.

### CONCLUDING REMARKS

General relations needed for the design of arbitrary cambered-span airfoils which will possess the theoretical minimum induced drag for specified flight conditions have been developed. These relations, however, allow the determination of the optimum wing form not only for minimum induced drag, but also for the maximum attainable value of lift-drag ratio by optimizing the chord distribution of the wing.

The procedures developed can be used for the determination of the optimum wing design when a specific spanwise camber line and section profile are given. The camber-line shape and wing section profile that will be best for a particular set of flight requirements depend, of course, upon the specific mission involved, and only by a series of comparative designs can the best overall wing form be determined in any particular case. The design procedures presented, however, are in a form which allows such efficiency comparisons to be easily made.

It should perhaps be explicitly emphasized that cambered-span wings will not in all cases possess superior aerodynamic efficiency compared with the optimum flat wing of equal projected span. The relative efficiencies of flat and curved wings will depend critically upon the ratio of the induced drag reduction to the increased profile drag of the cambered wing, and the magnitude of this ratio can be determined only by carrying out a series of comparative design analyses according to the methods presented herein.

The design procedure presented does not specifically include such possible effects as interference and tip separation drags. The method is based on the assumption that the two-dimensional sectional force coefficients are closely approximated by the profiles of the three-dimensional wings. For large span wings or wings with moderate spanwise camber, the procedure outlined should be quite valid within the limitations of linear lifting-line theory. The procedure also includes the assumption that the section profiles selected for wing construction have a sufficiently large minimum thickness that they will provide ample room for housing the wing spar structure.

The results of the illustrative comparison of a cambered wing with a flat wing of equal span (although neither wing has been optimized with respect to maximum lift-drag ratio) indicate that gains in operational efficiency can be secured with cambered-span wings, as compared with the efficiency of conventional wings currently in use, when use is made of special profiles to minimize the wing profile drag. The magnitudes of the gains attainable with cambered-span wings over

optimum flat wings will be smaller at low lift coefficients due to the predominance of the profile drag. At higher lift coefficients, however, where the induced drag becomes a significant factor in wing efficiency, the higher effective aspect ratio of cambered wings becomes very important for wings of limited span.

LANGLEY RESEARCH CENTER,  
 NATIONAL AERONAUTICS AND SPACE ADMINISTRATION,  
 LANGLEY STATION, HAMPTON, VA., June 5, 1962.

## APPENDIX A

### THE RELATIONSHIP OF LIFT TO INDUCED DRAG FOR OPTIMALLY LOADED AIRFOILS

It can be shown (ref. 1) that for any optimally loaded lifting line of projected span  $b'$  and producing a lift force  $L$ , the induced drag is given by

$$D_i = \frac{f}{q} \left[ \frac{L}{b'} \right]^2 \quad (A1)$$

where  $q$  is the free-stream dynamic pressure and  $f$  is a constant that depends only upon the shape of the spanwise camber line  $z(y)$ .

For a straight lifting-line segment, the circulation distribution is elliptical when the line is optimally loaded and

$$D_i = \frac{1}{\pi q} \left[ \frac{L}{b'} \right]^2 \quad (A2)$$

Therefore

$$f \text{ (straight line)} = \frac{1}{\pi} = 0.318 \quad (A3)$$

For a cambered-span airfoil (or any other non-planar lifting system), the induced drag is

$$D_i = \frac{1}{(BN_A)q} \left[ \frac{L}{b'} \right]^2 \quad (A4)$$

and

$$f \text{ (cambered line)} = \frac{1}{BN_A} \quad (A5)$$

From equation (4), when  $\psi = 1.0$  (corresponding to the condition where the projected spans of the straight and cambered wings are equal),

$$k = \pi^{-1} BN_A \quad (A6)$$

and the  $f$  value for any cambered form, when  $\psi = 1.0$  is used to determine  $k$ , is then given by

$$f \text{ (cambered line)} = \frac{1}{\pi k} = \frac{0.318}{k} \quad (A7)$$

When  $k > 1.0$ , the cambered span will possess less induced drag than the optimally loaded flat span. Thus, for wings of equal projected span, the induced drag depends only upon the total lift  $L$  and spatial distribution of the wake vorticity (whose effect is measured by  $f$ ), and is independent of wing area  $S$  or the associated aspect ratio  $A \left( = \frac{b'^2}{S} \right)$  so long as the wing loading is optimum.

The need to introduce a reference area  $S$  and aspect ratio  $A$  arises in defining coefficients.

### REFERENCES

1. Cone, Clarence D., Jr.: The Theory of Induced Lift and Minimum Induced Drag of Nonplanar Lifting Systems. NASA TR R-139, 1962.
2. Cone, Clarence D., Jr.: A Theoretical Investigation of Vortex-Sheet Deformation Behind a Highly Loaded Wing and Its Effect on Lift. NASA TN D-657, 1961.
3. Abbott, Ira H., and Von Doenhoff, Albert E.: Theory of Wing Sections. McGraw-Hill Book Co., Inc., 1949.
4. Abbott, Ira H., Von Doenhoff, Albert E., and Stivers, Louis S., Jr.: Summary of Airfoil Data. NACA Rep. 824, 1945. (Supersedes NACA WR L-560.)